Journal Pre-proof

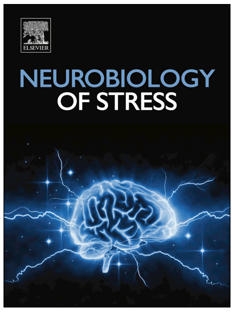

The antidepressant effect of nucleus accumbens deep brain stimulation is mediated by parvalbumin-positive interneurons in the dorsal dentate gyrus

Hong Zhou, Jiayu Zhu, Jie Jia, Wei Xiang, Hualing Peng, Yuejin Zhang, Bo Liu, Yangling Mu, Yisheng Lu

PII: S2352-2895(22)00067-4

DOI: https://doi.org/10.1016/j.ynstr.2022.100492

Reference: YNSTR 100492

To appear in: *Neurobiology of Stress*

Received Date: 13 June 2022

Revised Date: 2 September 2022

Accepted Date: 21 September 2022

Please cite this article as: Zhou H, Zhu J, Jia J, Xiang W, Peng H, Zhang Y, Liu B, Mu Y, Lu Y, The antidepressant effect of nucleus accumbens deep brain stimulation is mediated by parvalbumin-positive interneurons in the dorsal dentate gyrus, *Neurobiology of Stress* (2022), doi: https://doi.org/10.1016/j.ynstr.2022.100492.

Credit author statement

Hong Zhou and Jiayu Zhu: Conceptualization, Data curation, Formal analysis, Investigation, Methodology, Writing – original draft, Writing – review & editing, Software. Jie Jia, Wei Xiang, Hualing Peng and Yuejin Zhang: Formal analysis, Software. Bo Liu: Funding acquisition. Yangling Mu and Yisheng Lu: Conceptualization, Validation, Resources, Writing – review & editing, Supervision, Project administration, Funding acquisition.

Title Page

Title of article: The antidepressant effect of nucleus accumbens deep brain stimulation is mediated by parvalbumin-positive interneurons in the dorsal dentate gyrus

All authors' full names and e-mail addresses:

Hong Zhou[#1] 1121219557@qq.com ([#]contributed equally to this work)

Jiayu Zhu[#1] 1063578418@qq.com

Jie Jia[1] 358328020@qq.com

Wei Xiang[1] 1300636953@qq.com

Hualing Peng[1] 1982742815@qq.com

Yuejin Zhang[1] 1104585260@qq.com

Bo Liu[*4] dr.liubo@163.com

Yangling Mu[*1,2,3] ymu@hust.edu.cn

Yisheng Lu[*1,2,3] luys@hust.edu.cn ([*]Correspondence)

Author Affiliation:

[1]Department of Physiology, School of Basic Medicine, Tongji Medical College, Huazhong University of Science and Technology, Wuhan 430030, China

[2]Institute of Brain Research, Collaborative Innovation Center for Brain Science, Huazhong University of Science and Technology, Wuhan 430030, China

[3]Hubei Key Laboratory of Drug Target Research and Pharmacodynamic Evaluation, Huazhong University of Science and Technology, Wuhan 430030, China

[4]Department of Otorhinolaryngology, Union Hospital, Tongji Medical College, Huazhong University of Science and Technology, Wuhan 430022, China

Abstract

The nucleus accumbens (NAc) is a crucial region in the reward circuit and is related to anhedonia, the pivotal symptom of major depression disorder (MDD). Deep brain stimulation (DBS) of NAc has been identified as an effective treatment for severe refractory major depression; however, the underlying mechanism of NAc-DBS in MDD treatment remains elusive. Using the chronic unpredictable mild stress (CUMS) mouse model, we found NAc-DBS rescued depression-like behaviors, and reversed high gamma oscillation reduction and neurogenesis impairment in the dorsal dentate gyrus. Inactivation of parvalbumin (PV)-positive interneurons (PVI) in the dorsal DG led to depression-like behavior and decreased adult neurogenesis. Further investigation elucidated the VTA-DG GABAergic projection and CA1-NAc projection might jointly participate in NAc-DBS therapeutic mechanism. Disinhibition of the VTA-DG GABAergic projection had an antidepressant effect, and inhibition of the CA1-NAc projection reduced the antidepressant effect of DBS-NAc. Moreover, disinhibiting the VTA-DG GABAergic projection or activating the CA1-NAc projection could increase PV interneuron activity in the dorsal DG. These results showed PV interneurons in the dorsal DG as an essential target in depression and NAc-DBS antidepressant mechanisms.

Keywords: Deep brain stimulation, Depression, Dentate gyrus, Nucleus accumbens, Parvalbumin interneurons

1. Introduction

Major depression disorder (MDD) is the leading psychiatric disorder, affecting ~3.8% of the global population (Otte et al., 2016). Despite decades of research and development, approximately 30% of MDD patients do not respond to current medical and psychotherapeutic approaches, and around half of these cases are also not curable with noninvasive neurostimulation therapies like electroconvulsive therapy (Drobisz and Damborská, 2019; Nugent et al., 2020). These treatment-resistant depression (TRD) patients are more likely to endure psychosocial stress and commit suicide than non-resistant patients (Amital et al., 2008; Mrazek et al., 2014). Deep brain stimulation (DBS), which stimulates subcortical brain areas with implanted electrodes, is currently considered a legitimate invasive neurostimulation therapy for TRD (Drobisz and Damborská, 2019; Liu et al., 2020; Minichino et al., 2012; Williams et al., 2018).

The nucleus accumbens (NAc) is a crucial region in reward circuit and related to anhedonia (Nestler and Carlezon, 2006), and has been identified as a potential DBS target for TRD treatment (Drobisz and Damborská, 2019). The therapeutic effect of chronic NAc-DBS treatment was proved by the TRD patients without compromising cognitive functions (Bewernick et al., 2010; Bewernick et al., 2012; Grubert et al., 2011; Schlaepfer et al., 2008). NAc-DBS can also ameliorate chronic unpredictable mild stress (CUMS)-induced depression in the animal model, which might be due to reward circuitry activation (Hamani et al., 2014; Lim et al., 2015a; Lim et al., 2015b; Rummel et al., 2016). Medium spiny neurons (MSNs) are the primary type (~95%) of neurons in NAc, releasing GABA to the ventral tegmental area (VTA) and basolateral amygdala (BLA), two MDD linked brain regions (Al-Hasani et al., 2021; Jones et al., 2010). The NAc has two components, the core and the shell. The core of NAc receives dopaminergic projections from VTA and glutamatergic projections from BLA, prefrontal cortex, and hippocampus (Han et al., 2020; Li et al., 2018). Besides the local effects on the soma and non-neural tissue, NAc-DBS entrains the action potentials propagating through the efferent axons to the target brain regions, and through the afferent axons antidromically to the cell body in BLA, prefrontal cortex, and hippocampus (Jakobs et al., 2019). However, the neural circuit mechanism of the therapeutic effect is still largely unknown.

Considerable evidence suggests that hippocampus neurogenesis impairment is the leading cause of depression (Tunc-Ozcan et al., 2019). The hippocampus has a decreased volume in most MDD patients, which can be reversed by antidepressant or electroconvulsive treatments, indicating the hippocampus' role in MDD (Arnone et al., 2013; Bremner et al., 2000; Tendolkar et al., 2013). Neurogenesis malfunction might partially underpin the reduction of hippocampus volume in MDD patients (Boku et al., 2018). In the CUMS animal models, neural progenitor cell proliferation and survival in the dentate gyrus (DG) are diminished (Malberg et al., 2000), and enhanced neurogenesis in the DG is sufficient to cure depression in animal models (Hill et al., 2015). Adult neurogenesis is regulated by the local environment of the DG, especially parvalbumin (PV)-positive GABAergic interneurons (PVI) (Song et al., 2013). PVIs are fast-spiking neurons, targeting the soma and the initial segment of glutamate neurons (Song et al., 2013), thus dictating the excitatory-inhibitory balance and the oscillation in the brain regions (Cardin et al., 2009). CUMS-induced depression decreases PVI in the DG, and ablation of PVI can induce depression-like behavior, suggesting a causal relationship between PVI and depression (Chen et al., 2022). PVI is also crucial for hippocampal oscillation (Amilhon et al., 2015; Antonoudiou et al., 2020), and gamma oscillation reduction was proposed as a biomarker for depression (Fitzgerald and Watson, 2018).

In this study, we found that NAc-DBS treatment rescued depression-like behaviors induced by chronic unpredictable mild stress (CUMS), and abnormalities in the DG were also reversed. To further explore the antidepressant mechanism of NAc-DBS, neural circuit and local cellular mechanism of how NAc-DBS affects the dorsal DG were investigated.

2. Materials and Methods

2.1 Mice

A total of 195 adult male C57BL/6J mice and 38 adult PV-Cre were used in this study. C57BL/6J male mice were purchased from the Experimental Animals Center of Tongji Medical College, Huazhong University of Science and Technology. PV-Cre mice have been described previously and backcrossed with C57BL/6J for over 10 generations (Yi et al., 2020). Less than 5 mice were housed per cage (330 × 205 × 180 mm^3) at 22~24℃ and 55–80% humidity, on a schedule of 12:12 h light/dark cycle, with water and food available ad libitum. The cage change cycle was 7 days, the amount of corncob bedding used for mouse cages is 100g. The IACUC at Huazhong University of Science and Technology approved the animal procedures.

2.2. Experimental designs

Experiment 1 (Fig. S1A): To examine the effect of 2 weeks of chronic stress on anxiety- and depression-like behavior in mice, 52 eight-week-old mice were randomly divided into two groups, the control (n = 22) and CUMS (n = 30) group. The control group was domesticated normally and the CUMS group was exposed to two weeks of chronic stress. Behavior tests and body weight were assessed before and after the 2 weeks of chronic stress. Finally, blood samples and brain tissue from the two groups of mice were collected. The blood samples were processed for corticosterone measurements, the brains were processed for immunofluorescence analysis.

To examine the therapeutic effect of NAc-DBS on anxiety-depression-like mice, 59 eight-week-old mice were randomly divided into three groups, control (n = 22), DBS-off (n = 21) and DBS-on (n = 16) groups. The control group was fed normally. Mice in DBS-off and DBS-on groups were implanted with stimulating electrodes in the right NAc core one week before the CUMS protocol. After two weeks of chronic stress, the DBS-on group mice were treated with NAc-DBS for 1 week, but not DBS-off group. Behavior tests and body weight were assessed before and after the CUMS protocol of 2 weeks and after NAc-DBS treatment of 1 week. Finally, blood samples and brain tissue from the three groups of mice were collected. The blood samples were processed for corticosterone measurements, the brains were processed for immunofluorescence analysis.

Experiment 2 (Fig. S1B): To explore whether NAc-DBS could activate neurons in the DG through disinhibition of VTA GABAergic projection to the DG, 22 eight-week-old C57 mice were randomly divided into two groups, NaCl (n = 10) and CNO (n =11) groups, which were bilaterally co-injected with AAV-GAD67-Cre and AAV-DIO-hM4Di-mCherry viruses in VTA and implanted cannula in bilateral DG (Fig.5). Three weeks after virus injection, mice were anesthetized with isoflurane, and 1 μl CNO (1 μg/μl) or an equal volume of normal saline was bilaterally injected into the DG of CNO group or NaCl group mice through the cannula. After bilateral DG CNO- or NaCl-injection for 7 days, the animals were subjected to behavioral tests. Brains were then collected and processed for immunofluorescence analysis.

Experiment 3 (Fig. S1C): To explore whether CA1 to NAc projection can affect the treatment effect of NAc-DBS, 15 eight-week-old C57 mice were randomly divided into two groups, NaCl (n = 6) and CNO (n =9) groups. Retro-hSyn-tdTomato-P2A-iCre-WPRE-pA virus was injected into the right NAc and pAAV-EF1A-DIO-hM4Di-eGFP-WPRE virus was bilaterally injected into the dorsal hippocampal CA1 (Fig.6). Stimulating electrodes were implanted in the right NAc core of mice in CNO and NaCl groups. One weeks after virus injection, mice were exposed to chronic stress for 2 weeks. DBS treatment was performed 30 min after intraperitoneal injection of CNO or 0.9% NaCl solution in CNO or NaCl groups. Behavior tests were assessed before and after the CUMS protocol of 2 weeks and after NAc-DBS treatment of 1 week. Brains were then collected and processed for immunofluorescence analysis.

Experiment 4 (Fig. S1D): To activate CA1 to NAc projection, Retro-hSyn-tdTomato-P2A-iCre-WPRE-pA virus was injected into the right NAc and pAAV-EF1A-DIO-hM3Dq-eGFP-WPRE virus was bilaterally injected into the dorsal hippocampal CA1. 10 eight-week-old C57 mice were randomly divided into two groups, NaCl (n = 4) and CNO (n =6) groups. Three weeks after virus injection, mice in CNO or NaCl groups were intraperitoneally injected with CNO or 0.9% NaCl solution for 1 week. Brains were then collected and processed for immunofluorescence analysis.

2.3 CUMS

Mice were singly housed before CUMS protocol started. Briefly, this protocol consisted of four long-term stressors (for 24 h), including cage tilting, food or water deprivation, and placement in an empty cage, as well as seven short-term stressors: cold (4℃ for 1 h), white noise (1 h), hot (50℃ for 10 min), tail pinch (2 min), cage shaking (30 min), restraint (4 h), pepper smell (4 h). Each session randomly consisted of one long-term and two short-term stressors, with a two-hour break in between. One session was applied per day for 14 days.

2.4 DBS

Mice were anesthetized with 1% pentobarbital sodium (35 mg/kg, i.p.) and placed into a stereotaxic frame (RWD Life Science). Bipolar tungsten electrodes (795500, A-M System) were implanted into the right NAc core (coordinates: +1.1 mm anterior, +1.25 mm lateral, and -4.55 mm ventral to bregma). Mice were individually caged and recovered for a week after surgery. The electrical stimulation (130 Hz, 100 μA, and 60 μs pulse width) (AFG1022 Arbitrary Function Generator, Tektronix; ISO-flex stimulus isolator, A.M.P.I.) was given 1 h per day for seven days (Mayberg et al., 2005; Zhou et al., 2018). All the procedures were the same for control animals without the current application. The localization of the electrodes was confirmed by coronal sections after the experiment, data from animals with misplaced electrodes were excluded.

2.5 Stereotaxic Viral Injection

Adult mice were anesthetized with 1% pentobarbital sodium (35 mg/kg, i.p.) and head-fixed in a stereotaxic device (RWD life science; 68025). Using a glass pipette (Cetin et al., 2006), mice were injected with viruses (0.25 μL per side, 20 nL/min) at the NAc core (coordinates: +1.18 mm anterior, +1.25 mm lateral, and -4.55 mm ventral to bregma), DG (coordinates: -1.7 mm anterior, ±1.25 mm lateral, and −2.05 mm ventral to bregma), CA1 (coordinates: -1.94 mm anterior, ±1.25 mm lateral, and −1.5 mm ventral to bregma), and VTA (coordinates: -3.4 mm anterior, ±0.5 mm lateral, and −4.3 mm ventral to bregma) respectively. After injection, the glass pipette was left in place for 10 min before slowly removing it. Viruses used in this study are listed here: AAV-CAG-DIO-eGFP-2A-TetTox-pA (Taitool Bioscience, S0235-9, 2.08×10^{12} viral genomes (vg) per mL), AAV- EF1a-DIO-hM4Di-eGFP (Obio Technology, Shanghai, HYMBH15963, 5.18×10^{12} vg per mL), AAV-EF1a-DIO-eGFP (Obio Technology, Shanghai, H3303, 1.35×10^{13} vg per mL), Retro-hSyn-tdTomato-P2A-iCre-WPRE-pA (Taitool Bioscience, S0509-2R, 2.13×10^{13} vg per mL), AAV-GAD67-eGFP-2A-Cre-WPRE (Obio Technology, Shanghai, HYMBH10062, 2.39×10^{13} vg per mL), AAV-EF1a-DIO-hM3Dq-mCherry (Vigene Bioscience, Shandong, 4.39×10^{13} vg per mL), AAV-EF1a-DIO-hM4Di-mCherry (Vigene Bioscience, Shandong, 6.23×10^{13} vg per mL). Three weeks after virus injection, the animals were subjected to behavioral tests. Animals expressing hM3Dq or hM4Di were intraperitoneally injected with saline or Clozapine-N-oxide (CNO, 3 mg/kg, MCE) 30 min before the behavioral tests. Brains were sectioned afterward to verify the injection sites.

2.6 Behavioral Analysis

In all behavioral tests, adult mice (8-10 weeks) were employed. All mice were handled at least 10 min twice a day for 3 days before behavioral assays. All tests were performed during the light period, at 11:00 to 19:00 h, with the investigators unaware of the animal genotype and grouping information.

2.7 Open Field Test (OFT)

Mice were tested for their locomotor activity for 6 minutes in an opaque square open field area (45*45*45 cm), conceptually divided into the central field, the corner field, and the peripheral field. An automated video tracking system (Supermaze, Xinruan Information Technology Co. Ltd., Shanghai, China) was used to measure the distance traveled, average velocity, cumulative duration, entry frequency, and duration spent immobile in each field. After each trial, the apparatus was swept with 75% alcohol to avoid the presence of olfactory cues.

2.8 Tail Suspension Test (TST)

Mice were suspended gently approximately 50 cm above the table by their tails attached to a hook with adhesive tape, and the activity was videotaped (Xinruan Information Technology Co. Ltd., Shanghai, China). The immobile time was calculated by analyzing the 6 min test videotapes. Mice that climbed up their tails were excluded.

2.9 Sucrose Preference Test (SPT)

Mice were housed separately for 72 h before the experiment and given two bottles of water to drink for the first 24 h. Then one bottle of water was replaced with 1.5% (wt/vol) sucrose for the next 24 h, while the bottle positions were switched every 12 h. 24 h before the experiment, mice were denied fluid access. 30 min before the test, mice were anesthetized with isoflurane and were given 1 µl CNO (1 µg/µl) or saline bilaterally into the DG via cannula. For the next 4 h, mice were allowed access to both bottles, with positions switched every 2 h. Fluid consumption during the 4 h was measured. Then in the next 24 h, mice were allowed access to both bottles with positions switched every 12 h. Fluid consumption during the 24 h was measured. The sucrose preference was calculated as the sucrose preference (%) = sucrose consumption / (sucrose consumption + water consumption) (Fig. 5).

2.10 Corticosterone Measurements

Mice were anesthetized with 5% chloral hydrate, and blood samples were collected from the orbital sinus. Serum was isolated by clotting for 2 hours at room temperature and centrifugation at 1000 g for 20 min at 2~8℃. Corticosterone concentration was measured using the mouse corticosterone ELISA kit (Elabscience, Wuhan, China) according to the manufacturer's instructions. The optical density of each sample was measured at 450 nm using a microplate reader (TECAN Austria GmbH 5082 Grodig, Austria), and the corticosterone concentration was calculated by comparing the optical density of samples to the standard curve generated with the kit. All the assays were conducted within 3 h of receiving the serum samples.

2.11 Local Field Potential (LFP) recordings

Mice were anesthetized with pentobarbital sodium (35 mg/kg, i.p.) and mounted on a stereotaxic frame. Four tetrodes of four twisted Formvar-coated platinum-iridium probes (17 μm; California Fine Wire) were attached to a custom microdrive with Epoxy (Precision Fiber Products). The assembled microdrive was secured to the skull with the tetrodes targeted to the right DG (coordinates: -1.7 mm anterior, +1.25 mm lateral, and -2.05 mm ventral to bregma). All electrophysiological recordings were performed using the OmniPlex D Neural Data Acquisition System (Plexon Inc.). The electrical signal was digitized at 40 kHz after filtering at 0.05-8,000 Hz and amplified at a gain of 250-5,000. For the acute stress model induced by movement restriction, the LFP baseline in the dorsal DG was recorded three times within one hour for 5 minutes each time. The LFP was then recorded for 5 min at 0 min, 30 min and 55 min during the 1 h movement restriction by binding the limbs, and 0 min, 30 min and 55 min after the movement restriction. For the CUMS and DBS treatment models, the LFP in the dorsal DG was recorded for 5 min every day in the home cage and for 10 min every three days in the open field when the mice were not receiving stress treatments. After in vivo recordings and behavioral experiments, the electrode and cannula placements were verified by sectioning their brains. Mice were excluded if the implantation site was incorrect.

2.12 Immunofluorescence

Mice were anesthetized with 5% chloral hydrate and perfused transcranial with 0.1 M PBS followed by 4% PFA in 0.1 M PBS. The brain was removed and post-fixed overnight in 4% PFA at 4℃, then equilibrated in 30% sucrose. After being embedded in OCT, brain tissue was cut into 30 μm slices with a Leica cryostat or cooled-stage microtome and stored in 0.1 M PBS. In coronal sections, the dorsal dentate corresponded to AP coordinates −1.0 to −2.5 (in relation to bregma).

Take one slice out of every three slices and at least 5 slices per mouse were used for immunofluorescence. For BrdU injected mice brain, sections were incubated with 2 N HCl at 37℃ for 30 min, then neutralization with 0.1 M borate buffer for 10 min at room temperature. For immunostaining, sections were rinsed three times in trisphosphate buffer solution (TBS) and blocked with blocking buffer (3% BSA in TBS with 0.25% Triton X-100 and 10% goat serum) for 60 min at room temperature. Sections were then incubated at 4℃ overnight in blocking buffer containing the following primary antibodies: mouse anti-PV (A2791, Abclonal; 1:100), rabbit anti-Ki67 (ab15580, Abcam; 1:500), rat anti-BrdU (FITC conjugated; ab74545, Abcam; 1:300), rabbit anti-c-fos (ab214672, Abcam; 1:1000), mouse anti-NeuN (ab104224, Abcam; 1:1000). After washing with TBS three times, sections were incubated with secondary antibody in blocking buffer for 2 h at room temperature. The secondary antibodies were goat anti-rabbit IgG (ab150077, Abcam; 1:1000), goat anti-rat IgG (ab150157, ab150160, Abcam; 1:1000), goat anti-mouse IgG (ab150113, ab150116, Abcam; 1:1000). Washing with TBS three times, sections were mounted with mounting medium (containing DAPI) on glass slides, and images were taken using Olympus Fluoview FV1000 or Olympus VS120 slide scanning system. Image stacks of the DG area were compressed into a single plane using a maximum intensity projection. The number of fluorescent cells was counted by Image J 1.48v (National Institutes of Health, USA). A total of five images were analyzed per mouse, and each group contained at least 3 mice.

2.13 Statistical analysis

Data were analyzed with GraphPad Prism 7.00 (GraphPad Software) and Image-Pro Plus 6.0 (Media Cybernetics, Silver Spring, USA). Statistical differences between two groups were analyzed by applying the two-tailed Student's *t*-test. Data containing more than two groups were tested by using analysis of variance (ANOVA). Significant main effects or interactions were followed up with Tukey's post hoc test or Sidak's post hoc test. All data are expressed as the mean ± SEM. Statistical differences were considered when $p < 0.05$.

3. Result

3.1 NAc-DBS rescued depression-like behaviors induced by CUMS

After two weeks of chronic stress (Fig. S1A), the CUMS group demonstrated weight loss (Fig.1C, $t = 5.081$, df = 36, $p < 0.0001$), and increased immobile time in the TST (Fig. 1D, $t = 3.365$, df = 30, $p = 0.0021$). In the OFT, the CUMS group revealed lower locomotion activity (Fig. 1E, $t = 4.601$, df = 50, $p < 0.0001$), slower movement speed (Fig. 1F, $t = 4.599$, df = 50, $p < 0.0001$), avoiding the center (Fig. 1G, $t = 5.899$, df = 50, $p < 0.0001$) and preferring the corner (Fig. 1H, $t = 2.754$, df = 50, $p = 0.0082$). Serum corticosterone levels also increased in the CUMS group (Fig. 1I, $t = 4.793$, df = 20, $p = 0.0001$). These results indicated that mice exhibited anxiety- and depression-like behavior after CUMS treatment.

Then we elicited NAc-DBS to the CUMS treated mice for one week (Fig. S1A and Fig.1B). All the phenotypes of the CUMS group were rescued. Compared to the DBS-off group, mice in the DBS-on group showed weight gain (Fig. 1J, $F(2, 47) = 6.194$, $p = 0.0041$). In the TST, the immobile time was decreased in the DBS-on group in TST (Fig. 1 K, $F(2, 29) = 7.146$, $p = 0.003$). In the OFT, the locomotion activity of the DBS-on group recovered (Fig. 1L, $F(2, 38) = 6.731$, $p = 0.0031$), the movement speed rescued (Fig. 1M, $F(2, 38) = 6.788$, $p = 0.003$), the frequency of entering the center zone increased (Fig. 1N, $F(2, 38) = 7.435$, $p = 0.0019$), while the time spent in the corner zone decreased (Fig. 1O, $F(2, 38) = 5.395$, $p = 0.0087$). CUMS induced the elevation of serum corticosterone was likewise reversed by DBS treatment (Fig. 1P, $F(2, 39) = 21.29$, $p < 0.0001$). In addition, no significant difference between the control and the DBS-on groups in OFT and TST. These data indicated that NAc-DBS treatment could rescue the anxiety- and depression-like behavior induced by CUMS.

3.2 DBS reversed CUMS-induced high gamma oscillation reduction in the dorsal DG

First, we evaluated whether acute stress could induce hippocampus malfunction. We found that DG LFP power in theta (Fig. S2C, $t = 8.956$, df = 5, $p = 0.0003$), beta (Fig. S2D, $t = 3.512$, df = 5, $p = 0.0171$), and high gamma bands ((Fig. S2F, $t = 3.268$, df = 5, $p = 0.0222$) was reduced under acute restraint stress (Fig. S1). However, the power in all bands was recovered afterward, suggesting that acute stress might not be able to induce long-term hippocampus malfunction (Fig. S2). To evaluate whether CUMS could affect hippocampus function and be treated with NAc-DBS, DG LFP was recorded every day in the home cage (Fig. S2). The LFP power of the high gamma band was reduced in the home cage (Fig. 2A and E, $t = 3.213$, df = 16, $p = 0.0054$) after CUMS administration, but not in theta (Fig. 2B, $t = 0.7999$, df = 16, $p = 0.4355$), beta (Fig. 2C, $t = 0.042$, df = 16, $p = 0.9669$), and low gamma bands (Fig. 2D, $t = 1.18$, df = 16, $p = 0.2554$). After NAc-DBS treatment, the high gamma band (Fig I, $F(2, 21) = 5.577$, $p = 0.0114$) power of LFP in the DBS-on group was recovered in the home cage compared to the DBS-off group (Fig. F-I). These results suggest that high gamma band power in the DG is correlated with CUMS-induced depression behaviors, which can be reversed by NAc-DBS treatment (Fig. 2).

3.3 DBS reversed CUMS-induced neurogenesis impairment and PVI loss in the dorsal DG

To explore whether adult neurogenesis abnormalities in the DG after CUMS may be reversed by NAc-DBS, Ki67 was utilized as a proliferation marker and BrdU was employed as a marker of neural progenitor cell survival (Fig. 3A and B). Consistent with the literature, both Ki67 (Fig. 3C, $t = 9.251$, df = 9, $p < 0.0001$) and BrdU-positive cells (Fig.3E, $t = 4.25$, df = 6, $p = 0.0054$) were significantly reduced in the dorsal DG by CUMS; and NAc-DBS restored the amount of Ki67 (Fig. 3D, $F(2, 9) = 20.09$, $p = 0.0005$) and BrdU-positive cells (Fig. 3F, $F(2, 12) = 10.08$, $p = 0.0027$) in the DG, suggesting that DBS treatment increased adult neurogenesis in the dorsal DG of the CUMS-induced depression-like mouse model.

PVIs are required for hippocampal gamma oscillation (Antonoudiou et al., 2020; Bezaire et al., 2016; Gulyás et al., 2010), and these PVI are also essential for adult neurogenesis (Song et al., 2013). Whether PVI in the hippocampus can be affected by CUMS and be reversible by DBS needs investigation. We found the number of PVI reduced significantly in the DG of CUMS-induced depression mice (Fig. 4A and B, $t = 4.366$, df = 15, $p = 0.0006$), which was recovered by NAc-DBS (Fig. 4A and C, $F(2, 22) = 7.973$, $p = 0.0025$), suggesting NAc-DBS might reverse the behavior phenotypes, gamma oscillation and neurogenesis impairment in the DG through promoting PVI.

3.4 Inhibition of PVI in the DG induced depression-like behaviors

To investigate whether impairment of PVI in the DG plays a key role in inducing anxiety- and depression-like behavior in mice, we used tetanus toxin (TetTox) to inhibit GABA release of PVI in the dorsal DG (Fig. 4D). Cre-dependent AAV-CAG-DIO-eGFP-2A-TetTox or AAV-CAG-DIO-eGFP was bilaterally injected into the dorsal DG of PV-Cre mice (PV-TetTox mice or PV-eGFP mice) (Fig. 4D). Cre-dependent expression of eGFP was confirmed by immunofluorescence staining. The PV-positive interneurons in the dorsal DG were co-localized with eGFP-positive cells (Fig. 4E). Three weeks after virus injection, the immobile time of PV-TetTox group mice increased significantly in TST (Fig. 4F, $t = 2.321$, df = 13, $p = 0.0371$). In the OFT (Fig. 4G-I), the PV-TetTox group mice revealed avoiding the center (Fig. 4I, $t = 3.149$, df = 13, $p = 0.0077$) and preferring the corner (Fig. 4J, $t = 5.497$, df = 13, $p = 0.0001$). The results suggested that blocking the GABA release of PV-interneuron in the dorsal DG could induce anxiety- and depression-like behaviors.

To examine whether inhibition of PVI's activity in the dorsal DG can induce anxiety- and depression-like behaviors, the AAV-EF1A-DIO-hM4Di-eGFP or AAV-EF1A-DIO-eGFP virus was bilaterally injected into the dorsal DG of PV-Cre mice for three weeks (Fig. 4K), animals with AAV-EF1A-DIO-hM4Di-eGFP virus were randomly divided into two groups, one group injected with 0.9% NaCl solution (NaCl group) and the other injected with clozapine-N-oxide (CNO; CNO group). Animals with AAV-EF1A-DIO-eGFP virus were injected with the same concentration of CNO (eGFP group). Cre-dependent expression was confirmed by immunofluorescence staining (Fig. 4L). The behaviors were tested after CNO (3 mg/kg) or 0.9% NaCl intraperitoneally injection once a day for 7 days. Compared to eGFP group and NaCl group mice, the immobile time of CNO treatment group mice increased significantly in TST (Fig. 4M, $F(2, 20) = 7.328$, $p = 0.0041$). In OFT (Fig. 4N-Q), CNO treatment decreased the total distance traveled (Fig. 4N, $F(2, 20) = 7.501$, $p = 0.0037$), the movement speed (Fig. 4O, $F(2, 20) = 7.5$, $p = 0.0037$) and the frequency of center zone entry (Fig. 4P, $F(2, 20) = 9.71$, $p = 0.0011$), and increased the time in the corner zone significantly (Fig. 4Q, $F(2, 20) = 17$, $p < 0.0001$). The results suggested that inhibited PVI activity in the dorsal DG also could induce anxiety- and depression-related behaviors in mice. Therefore, our data demonstrated that PVI in the dorsal DG plays a vital role in depression.

3.5 Inhibition of PVI in the dorsal DG decreased newborn cells

PVIs promote newborn progenitors proliferating, survival and maturation in the adult DG (Song et al., 2013); we analyzed adult neurogenesis by immunofluorescence staining for Ki67 and BrdU (Fig. 4R-U). The number of ki67 (Fig. 4V, $t = 9.188$, df =9, $p < 0.0001$) and BrdU positive neurons (Fig. 4W, $t = 11.99$, df =7, $p < 0.0001$) in the dorsal DG of PV-TetTox mice was less than that of PV-eGFP mice. For AAV-EF1A-DIO-hM4Di-eGFP or AAV-EF1A-DIO-eGFP virus dorsal DG injected mice, after being injected with CNO (3 mg/kg) or 0.9% NaCl solution intraperitoneally for 7 days, the number of ki67 (Fig. 4X, F(2, 12) = 10.25, p = 0.0025) and BrdU positive neurons (Fig. 4Y, F(2, 6) = 8.057, p = 0.02) in the dorsal DG of CNO group mice was less than that of NaCl and eGFP groups mice. These results indicate that adult neurogenesis and the survival of NSCs were decreased in the dorsal DG of mice with dysfunction of PVI, which might induce anxiety- and depression-related behaviors in mice.

3.6 Disinhibition of the VTA-DG GABAergic projection has an antidepressant effect

After NAc-DBS treatment, the dorsal hippocampal neuronal activity was analyzed by immunofluorescence staining for c-fos and NeuN. The number of NeuN+ and c-fos+ neurons in the dorsal hippocampal DG (Fig. S4D, t = 3.215, df =8, p = 0.0123), CA1(Fig. S4E, t = 4.216, df =5, p = 0.0084) and CA3 was significantly increased in the DBS-on group mice (Fig. S4A-E). Statistical analysis demonstrated that the number of c-fos+ and PVI in the dorsal DG of DBS-on group mice was increased (Fig. S4F and G, t = 4.049, df =9, p = 0.0029). MSN neurons in NAc are mostly GABAergic neurons, directly targetting VTA GABAergic neurons via $GABA_A$ receptors (Xia et al., 2011) and the VTA GABAergic axons make synaptic contacts in the granule cell layer of the dentate gyrus (Ntamati and Lüscher, 2016). To analyze VTA GABAergic neuron activity after NAc-DBS treatment, we injected bilateral VTA with AAV-GAD67-eGFP virus to label GABAergic neurons, followed by immunostaining for c-fos (Fig. S5A-C). Statistical analysis demonstrated that the number of c-fos+ and GAD67+ in the VTA of DBS-on group mice was decreased (Fig. S5D, t = 3.903, df =5, p = 0.0114). Therefore, we speculate that NAc-DBS could activate neurons in the DG through disinhibition of VTA GABAergic projection to the DG.

Accordingly, bilateral co-injection of the AAV-GAD67-Cre and AAV-DIO-hM4Di-mCherry viruses into the VTA enables the expression of the Gi-coupled inhibitory hM4Di receptor in GAD67+-neurons (Fig. 5A and D), while the bilateral DG-injection of CNO guarantees the selective silence of the GABAergic projection from VTA to DG (Fig. 5A-D). After bilateral DG CNO-injection for 7 days, the immobile time in TST was reduced (Fig. 5E, t = 4.119, df = 19, p = 0.0006) and the sucrose preference was increased in SPT in 4 hours (Fig. 5F, t = 2.81, df = 19, p = 0.0112). However, in the next 24 hours, there was no significant difference between the two groups in sucrose preference, which might be due to the degradation of CNO (Fig. 5G, t = 1.088, df = 19, p = 0.2904).

In the OFT (Fig. 5H-K), the bilateral DG CNO-injection mice avoided the center zone (Fig. 5J, t = 2.497, df = 19, p = 0.0219). These data indicated that inactivating the GABAergic projection from VTA to DG may have an anti-depressant effect but promote anxiety. Similarly, the number of ki67 (Fig. 5M, t = 6.094, df = 8, p = 0.0003) and BrdU positive cells (Fig. 5O, t = 8.129, df = 6, p = 0.0002) in the dorsal DG of mice injected with CNO was more than that of mice injected with 0.9% NaCl solution (Fig. 5L-O). The number of c-fos+ and PVI co-labeled cells in the dorsal DG of mice injected with CNO was also increased than that of mice injected with 0.9% NaCl solution (Fig. 5P and Q, t = 2.702, df = 8, p = 0.027). However, no significant difference was observed after activation of GABAergic projection from VTA to DG, through bilateral co-injection of the AAV-GAD67-Cre and AAV-DIO-hM3Dq-mCherry viruses (Fig. S6A-D) into the VTA with bilateral DG-injection of CNO (Fig. S6E-K).

3.7 NAc-DBS therapeutic effect for depression requires CA1 to NAc projection

NAc receives glutamatergic projections from the dorsal hippocampus CA1 (dCA1), to regulate this projection, Retro-hSyn-tdTomato-P2A-iCre-WPRE-pA virus was injected into the right NAc and pAAV-EF1A-DIO-hM4Di-eGFP-WPRE virus was bilaterally injected into the dorsal hippocampal CA1 (Fig. 6A-D). DBS treatment was performed 30 min after intraperitoneal injection of CNO or 0.9% NaCl solution. Compared to DBS-on with 0.9% NaCl solution, the immobile time of DBS-on with CNO group mice was significantly increased in TST (Fig. 6E). Two-way ANOVA revealed a significant CNO treatment × depression-like behavior interaction (F(2,26) = 5.037, p = 0.0142), Tukey's *post hoc* test showed significant difference between Control and CUMS in NaCl group (p = 0.0067) and in CNO group (p = 0.0004), CUMS and DBS in NaCl group (p = 0.0042), Control and DBS in CNO group (p = 0.0006); Sidak's *post hoc* test also showed significant difference between NaCl group and CNO group after DBS treatment (p = 0.0007). The result noted that inhibition of CA1-NAc projections during NAc-DBS treatment could not reverse the immobile time of TST in the CNO group, suggesting the NAc-DBS effect requires the activity of CA1-NAc projection. Similarly, in the OFT, the therapeutic effect of DBS for anxiety behavior was abolished by CNO injection (Fig. 6F-I). The DBS on with CNO group mice still revealed slower motion ability in the OFT (Fig. 6F). Two-way ANOVA revealed a significant CNO treatment × anxiety- and depression-like behavior interaction (F(2,26) = 3.98, p = 0.031), Tukey's *post hoc* test showed significant difference between Control and CUMS in NaCl group (p = 0.0033) and in CNO group (p = 0.0012), CUMS and DBS in NaCl group (p = 0.0395), Control and DBS in CNO group (p = 0.0001). In the OFT, the DBS on with CNO group mice still showed slower motion ability slower movement speed (Fig. 6G). Two-way ANOVA revealed a significant CNO treatment × anxiety-like behavior interaction ($F(2,26)$ = 3.99, p = 0.0308), Tukey's *post hoc* test showed significant difference between Control and CUMS in NaCl group (p = 0.0033) and in CNO group (p = 0.0012), CUMS and DBS in NaCl group (p = 0.0391), Control and DBS in CNO group (p = 0.0001). In the OFT, the DBS on with CNO group mice still revealed avoiding the center (Fig. 6H). Two-way ANOVA revealed a significant CNO treatment × anxiety-like behavior interaction ($F(2,26)$ = 3.883, p = 0.0335), Tukey's *post hoc* test showed significant difference between CUMS and DBS in NaCl group (p = 0.0403), Control and DBS in CNO group (p = 0.011). In the OFT, the DBS on with CNO group mice still showed preferring the corner (Fig. 6I). Two-way ANOVA, Sidak's *post hoc* test showed significant difference between NaCl group and CNO group after DBS treatment (p = 0.0249). These results suggested the CA1-NAc projection activation is required for NAc-DBS treatment. Then we analyzed adult neurogenesis by immunofluorescence staining for Ki67 and BrdU. The number of ki67 (Fig.6L, t = 3.545, df = 6, p = 0.0121) and BrdU positive cells (Fig.6M, t = 2.65, df = 7, p = 0.0329) in the dorsal DG of DBS-on with CNO group mice was less than that of NaCl group mice (Fig. 6J-M). This further suggests that NAc-DBS beneficial effect on neurogenesis in the DG also requires CA1-NAc projection. To activate this projection, Retro-hSyn-tdTomato-P2A-iCre-WPRE-pA virus was injected into the right NAc and pAAV-EF1A-DIO-hM3Dq-eGFP-WPRE virus was bilaterally injected into the dorsal hippocampal CA1 (Fig. S7A-C). We found that more c-fos+ and PVI co-labeled cells in the dorsal DG of CNO group mice than that of NaCl group mice (Fig. S7D and E, t = 2.772, df = 8, p = 0.0242).

4. Discussion

Gamma rhythms have been proposed as a biomarker or endophenotype in major depressive disorder (Fitzgerald and Watson, 2018). Under certain conditions gamma rhythms could distinguish subjects with major depression from healthy controls (Lee et al., 2010; Liu et al., 2014; Strelets et al., 2007). Clinical studies have found that high gamma power could be used as a marker to identify suicidal patients with depression (Arikan et al., 2019). For animal models, mice in depression-like behavior showed deficits in gamma signaling (Sauer et al., 2015). In addition to being associated with depressive states, gamma rhythms are more relevant to antidepressant treatment. Several studies have found increases in gamma signaling after recovery from depression(Noda et al., 2017; Pathak et al., 2016). Noda et al showed that treatment recovery in major depressive disorder was associated with an increase in prefrontal gamma power (Noda et al., 2017). Gamma rhythms were causal with respect to the therapeutic actions of ketamine and monoaminergic antidepressants (Alaiyed et al., 2019; Shaw et al., 2015). Likewise, nonpharmacological treatments for depression using transcranial magnetic stimulation (TMS) have identified gamma rhythm as the key indicator of treatment success(Noda et al., 2017). A mouse model of CRS-induced depression showed restoration of gamma activity at the network level is associated with behavioral remission(Khalid et al., 2016). These are consistent with our findings that NAc-DBS treatment of depression could restore changes in high gamma oscillations. It is known that gamma oscillations reflect the rhythmic firing of inhibitory interneurons, especially PVI.

Stress can disrupt the function of GABA in the hippocampal. Numerous studies suggested that the GABA levels were reduced in MDD subjects and stressed rodents. Early-life stress in rats led to an increase and a decrease in hippocampal glutamate and GABA release, respectively (Martisova et al., 2012). The role of GABAergic interneurons, mainly somatostatin- and parvalbumin-expressing cells, is required for the optimal E: I balance, which the malfunction of these cells can result in depression-related behaviors (Fogaça and Duman, 2019). A number of studies have demonstrated that PVI are involved in the pathogenesis of depression. Hippocampal PVI function is impaired in depression (Holm et al., 2011). Several animal studies have found that the number or density of PVI in the hippocampus is significantly decreased in various animal models of depression(Csabai et al., 2017; Czéh et al., 2015; Filipović et al., 2013). Cze´ h et al. (2005) showed that nine weeks of daily chronic mild stress resulted in a reduction of PVI in all subregions of the dorsal hippocampus (Czeh et al., 2005). Chronic mild stress induced a decrease in PVI in the hippocampus, whereas CCK and calbindin expression remained unchanged (Czéh et al., 2015; Filipović et al., 2013). Chronic social isolation induced depression animal model also shows a PVI decrease in the dorsal hippocampus, representing a high vulnerability of specific hippocampal interneurons to excitotoxic injury (Nullmeier et al., 2011; Perić et al., 2019). Overall, a reduced number of these PVI in the hippocampal subregions may consequently decrease the GABA release leading to excessive glutamate release, which might induce hippocampal hyperexcitability. PVI also play an important role in the treatment of depression (Möhler, 2012). Studies showed that four weeks of Flx treatment at the dose of 15 mg/kg/day attenuated the five-week psychosocial stress-induced decrement of hippocampal PVI in the DG (Czeh et al., 2005). Long-term administration of Flx or Clz might provide protection against CSIS by modulating the hippocampal GABAergic system, contributing to their therapeutic effect in mood disorders (Filipović et al., 2018). Running exercise regulated PVI through PGC-1α in the hippocampus of mice to reverse depressive-like behaviors (Wang et al., 2021). Acute chemogenetic activation of PVI in the DG produced anxiolytic-like behavior although it did not affect depressive-like behavior in the tail-suspension test (Zou et al., 2016). Therefore, PVI are a potential target for the treatment of depressive and anxiety disorders.

Studies have found that parvalbumin interneuron activation alters stem cell quiescence and progenitor proliferation, promotes newborn GC survival and maturation, while suppressed PVI activity decreases the survival and maturation of newborn neurons (Song et al., 2013; Song et al., 2012). PVI mediate slow spillover signaling and spillover transmission mediates activity-dependent regulation of early events in adult neurogenesis (Vaden et al., 2020). Ablation of ErbB4 in parvalbumin-positive interneurons inhibits adult hippocampal neurogenesis (Zhang et al., 2018). Running to reverse schizophrenia-like phenotypes relies on parvalbumin interneuron activation-dependent adult hippocampal neurogenesis (Yi et al., 2020). In the present research, our data suggested that inhibited PVI in the dorsal DG reduced adult neurogenesis and resulted in anxiety- and depression-like behavior in mice. Newborn neurons mature and form functional synapses with their efferent targets from CA2 and CA3 pyramidal neurons, and receive synaptic information from the perforant pathway and inhibitory interneurons (Alvarez et al., 2016; Yi et al., 2020). Therefore, these newborn neurons are pivotal for the normal function of the DG, and any impairment in their survival and maturation will induce various depression-related emotional disorders.

Deep brain stimulation (DBS), as an adjustable and reversible method for the regulation of local neural pathway activity, is used to treat a lot of neurologic and psychiatric disorders including depression (Altinay et al., 2015; Drobisz and Damborská, 2019). The NAc is known for its central role in pleasure and reward. Studies have found that the activation of the NAc increased for a presented reward and decreased for a punishment (Wacker et al., 2009). The possibility of stimulating the NAc has been verified in several studies. NAc-DBS decreases ratings of depression and anxiety in treatment-resistant depression (Bewernick et al., 2010). Four-year data on NAc-DBS have indicated a stable antidepressant and anxiolytic effect in the group of 11 patients suffering from treatment-resistant depression (Schlaepfer et al., 2008). In the present study, NAc-DBS treatment for one week could rescue the anxiety and depression-like behavior in CUMS mice. And we found the direct projection of dCA1-NAc and the indirection of NAc-VTA-DG might jointly participate in this therapeutic mechanism.

Both the hippocampus and NAc play important roles in reward-related behaviors. The CA1 region of the hippocampus contributes most of the long-range inputs to the NAc, especially projects to the NAc shell (Li et al., 2018). Recently a study has indicated that the dCA1 selectively projected excitatory glutamatergic inputs to the NAc shell (Liu et al., 2021). Chemogenetic and optogenetic inactivation of the dCA1-NAc shell pathway decreased the recurrence of long- and short-term morphine-paired context memory in mice (Liu et al., 2021). Our present data showed that there was a significant increase in the number of c-fos in the dCA1 region of the DBS-on mice (Fig. S3). Chemogenetic inactivation of the dCA1-NAc pathway reduced the therapeutic effect of NAc-DBS on anxiety-depression-related behaviors in mice (Fig. 6). These results indicated dCA1-NAc was one of the pathways that affect the therapeutic effect of NAc-DBS on CUMS depression model.

The VTA is a heterogeneous structure, makeup of dopamine, GABA, and glutamate neurons (Miranda-Barrientos et al., 2021). Recently study found that a subset of NAc MSNs directly targets non-dopaminergic VTA neurons, and these MSN GABAergic terminals are sensitive to opioids and mediate by $GABA_A$ receptors (Xia et al., 2011). GABA neurons constitute about 35% of neurons in the VTA and their axons make synaptic contacts in the granule cell layer of the DG (Ntamati and Lüscher, 2016). Therefore NAc-VTA-DG would form a disinhibition projection, which is an indirect projection of NAc to the hippocampus. There is evidence that the GABA neurons in VTA are robustly activated by stress or aversive stimuli, which to a certain extent are consistent with our results (Bouarab et al., 2019; Cohen et al., 2012). Therefore, we tented to think that the projection of dCA1-NAc and NAc-VTA-dorsal DG worked together in NAc-DBS treatment. This study deepens our understanding of the treatment mechanism of DBS and provides new ideas and treatment targets for depression.

5. Conclusions

In summary, the present study provides evidence for PVI in the dorsal DG are involved in regulating the antidepressant effect of NAc-DBS. As shown in Fig. 7, the NAc-DBS rescued depression-like behaviors induced by CUMS, reversed high gamma oscillation reduction, neurogenesis impairment and PV neuron loss in the dorsal DG. Blocking the GABA release of PVI in the dorsal DG could induce anxiety-depression-like behaviors and decreased adult neurogenesis. Furthermore, we explore the neural circuit of NAc-DBS antidepressants. We found the CA1-NAc projection and VTA-DG GABAergic projection may jointly participate in NAc-DBS therapeutic mechanism. Inhibition of the CA1-NAc projection reduced the antidepressant effect of DBS-NAc, and disinhibition of the VTA-DG GABAergic projection has an antidepressant effect, which both were involved in the activity of PV interneuron in the dorsal DG.

However, the neural circuit mechanism needs to be further explored. NAc-DBS may also affect dDG PVI activity through other brain regions, including prefrontal cortex and amgydala. How CA1-NAc projection and NAc-VTA-DG projection affect PVI in the DG is still quite unclear, which requires further investigation. In general, this work gives us a relatively novel understanding of the therapeutic mechanism of NAc-DBS and hopes to shed light on understanding depression pathogenesis and developing putative interventions.

6. Data Availability Statement

All datasets generated for this study are included in the article/supplementary material.

7. Ethics Statement

The animal study was reviewed and approved by the Animal Welfare Committee of Huazhong University of Science and Technology.

8. Credit authorship contribution statement

Hong Zhou and Jiayu Zhu: Conceptualization, Data curation, Formal analysis, Investigation, Methodology, Writing – original draft, Writing – review & editing, Software. Jie Jia, Wei Xiang, Hualing Peng and Yuejin Zhang: Formal analysis, Software. Bo Liu: Funding acquisition. Yangling Mu and Yisheng Lu: Conceptualization, Validation, Resources, Writing – review & editing, Supervision, Project administration, Funding acquisition.

9. Declaration of competing interest

The authors declare no conflict of interest.

10. Funding

This work was supported by the National Natural Science Foundation of China (82071508, 81670930).

11. Acknowledgments

The authors wish to thank Guangpin Chu, Xueling Lin, Juan Luo, Linlin Gao and Yuanlong Song for their support.

12. Reference

Al-Hasani, R., Gowrishankar, R., Schmitz, G.P., Pedersen, C.E., Marcus, D.J., Shirley, S.E., Hobbs, T.E., Elerding, A.J., Renaud, S.J., Jing, M., *et al.* (2021). Ventral tegmental area GABAergic inhibition of cholinergic interneurons in the ventral nucleus accumbens shell promotes reward reinforcement. Nat Neurosci *24*, 1414-1428.

Alaiyed, S., Bozzelli, P.L., Caccavano, A., Wu, J.Y., and Conant, K. (2019). Venlafaxine stimulates PNN proteolysis and MMP-9-dependent enhancement of gamma power; relevance to antidepressant efficacy. Journal of neurochemistry *148*, 810-821.

Altinay, M., Estemalik, E., and Malone, D.A., Jr. (2015). A comprehensive review of the use of deep brain stimulation (DBS) in treatment of psychiatric and headache disorders. Headache *55*, 345-350.

Alvarez, D.D., Giacomini, D., Yang, S.M., Trinchero, M.F., Temprana, S.G., Büttner, K.A., Beltramone, N., and Schinder, A.F. (2016). A disynaptic feedback network activated by experience promotes the integration of new granule cells. Science (New York, NY) *354*, 459-465.

Amilhon, B., Huh, C.Y., Manseau, F., Ducharme, G., Nichol, H., Adamantidis, A., and Williams, S. (2015). Parvalbumin Interneurons of Hippocampus Tune Population Activity at Theta Frequency. Neuron *86*, 1277-1289.

Amital, D., Fostick, L., Silberman, A., Beckman, M., and Spivak, B. (2008). Serious life events among resistant and non-resistant MDD patients. J Affect Disord *110*, 260-264.

Antonoudiou, P., Tan, Y.L., Kontou, G., Upton, A.L., and Mann, E.O. (2020). Parvalbumin and somatostatin interneurons contribute to the generation of hippocampal gamma oscillations. Journal of Neuroscience *40*, 7668-7687.

Arikan, M.K., Gunver, M.G., Tarhan, N., and Metin, B. (2019). High-Gamma: A biological marker for suicide attempt in patients with depression. Journal of affective disorders *254*, 1-6.

Arnone, D., McKie, S., Elliott, R., Juhasz, G., Thomas, E.J., Downey, D., Williams, S., Deakin, J.F., and

Anderson, I.M. (2013). State-dependent changes in hippocampal grey matter in depression. Molecular psychiatry *18*, 1265-1272.

Bewernick, B.H., Hurlemann, R., Matusch, A., Kayser, S., Grubert, C., Hadrysiewicz, B., Axmacher, N., Lemke, M., Cooper-Mahkorn, D., Cohen, M.X.*, et al.* (2010). Nucleus accumbens deep brain stimulation decreases ratings of depression and anxiety in treatment-resistant depression. Biol Psychiatry *67*, 110-116.

Bewernick, B.H., Kayser, S., Sturm, V., and Schlaepfer, T.E. (2012). Long-term effects of nucleus accumbens deep brain stimulation in treatment-resistant depression: evidence for sustained efficacy. Neuropsychopharmacology *37*, 1975-1985.

Bezaire, M.J., Raikov, I., Burk, K., Vyas, D., and Soltesz, I. (2016). Interneuronal mechanisms of hippocampal theta oscillations in a full-scale model of the rodent CA1 circuit. Elife *5*, e18566.

Boku, S., Nakagawa, S., Toda, H., and Hishimoto, A. (2018). Neural basis of major depressive disorder: Beyond monoamine hypothesis. Psychiatry and clinical neurosciences *72*, 3-12.

Bouarab, C., Thompson, B., and Polter, A.M. (2019). VTA GABA Neurons at the Interface of Stress and Reward. Frontiers in neural circuits *13*, 78.

Bremner, J.D., Narayan, M., Anderson, E.R., Staib, L.H., Miller, H.L., and Charney, D.S. (2000). Hippocampal volume reduction in major depression. The American journal of psychiatry *157*, 115-118.

Cardin, J.A., Carlén, M., Meletis, K., Knoblich, U., Zhang, F., Deisseroth, K., Tsai, L.H., and Moore, C.I. (2009). Driving fast-spiking cells induces gamma rhythm and controls sensory responses. Nature *459*, 663-667.

Cetin, A., Komai, S., Eliava, M., Seeburg, P.H., and Osten, P. (2006). Stereotaxic gene delivery in the rodent brain. Nature protocols *1*, 3166-3173.

Chen, S., Chen, F., Amin, N., Ren, Q., Ye, S., Hu, Z., Tan, X., Jiang, M., and Fang, M. (2022). Defects of parvalbumin-positive interneurons in the ventral dentate gyrus region are implicated depression-like behavior in mice. Brain, behavior, and immunity *99*, 27-42.

Cohen, J.Y., Haesler, S., Vong, L., Lowell, B.B., and Uchida, N. (2012). Neuron-type-specific signals for reward and punishment in the ventral tegmental area. Nature *482*, 85-88.

Csabai, D., Seress, L., Varga, Z., Ábrahám, H., Miseta, A., Wiborg, O., and Czéh, B. (2017). Electron Microscopic Analysis of Hippocampal Axo-Somatic Synapses in a Chronic Stress Model for Depression. Hippocampus *27*, 17-27.

Czeh, B., Simon, M., Van Der Hart, M.G., Schmelting, B., Hesselink, M.B., and Fuchs, E. (2005). Chronic stress decreases the number of parvalbumin-immunoreactive interneurons in the hippocampus: prevention by treatment with a substance P receptor (NK 1) antagonist. Neuropsychopharmacology *30*, 67-79.

Czéh, B., Varga, Z.K.K., Henningsen, K., Kovács, G.L., Miseta, A., and Wiborg, O. (2015). Chronic stress reduces the number of GABAergic interneurons in the adult rat hippocampus, dorsal-ventral and region-specific differences. Hippocampus *25*, 393-405.

Drobisz, D., and Damborská, A. (2019). Deep brain stimulation targets for treating depression. Behav Brain Res *359*, 266-273.

Filipović, D., Stanisavljević, A., Jasnić, N., Bernardi, R.E., Inta, D., Perić, I., and Gass, P. (2018). Chronic Treatment with Fluoxetine or Clozapine of Socially Isolated Rats Prevents Subsector-Specific Reduction of Parvalbumin Immunoreactive Cells in the Hippocampus. Neuroscience *371*, 384-394.

Filipović, D., Zlatković, J., Gass, P., and Inta, D. (2013). The differential effects of acute vs. chronic stress and their combination on hippocampal parvalbumin and inducible heat shock protein 70 expression. Neuroscience *236*, 47-54.

Fitzgerald, P.J., and Watson, B.O. (2018). Gamma oscillations as a biomarker for major depression: an emerging topic. Transl Psychiatry *8*, 177.

Fogaça, M.V., and Duman, R.S. (2019). Cortical GABAergic dysfunction in stress and depression: new insights for therapeutic interventions. Frontiers in cellular neuroscience *13*, 87.

Grubert, C., Hurlemann, R., Bewernick, B.H., Kayser, S., Hadrysiewicz, B., Axmacher, N., Sturm, V., and Schlaepfer, T.E. (2011). Neuropsychological safety of nucleus accumbens deep brain stimulation for major depression: effects of 12-month stimulation. The world journal of biological psychiatry : the official journal of the World Federation of Societies of Biological Psychiatry *12*, 516-527.

Gulyás, A.I., Szabó, G.G., Ulbert, I., Holderith, N., Monyer, H., Erdélyi, F., Szabó, G., Freund, T.F., and Hájos, N. (2010). Parvalbumin-containing fast-spiking basket cells generate the field potential oscillations induced by cholinergic receptor activation in the hippocampus. Journal of Neuroscience *30*, 15134-15145.

Hamani, C., Amorim, B.O., Wheeler, A.L., Diwan, M., Driesslein, K., Covolan, L., Butson, C.R., and Nobrega, J.N. (2014). Deep brain stimulation in rats: different targets induce similar antidepressant-like effects but influence different circuits. Neurobiology of disease *71*, 205-214.

Han, S., Cui, Q., Wang, X., Chen, Y., Li, D., Li, L., Guo, X., Fan, Y.S., Guo, J., Sheng, W.*, et al.* (2020). The anhedonia is differently modulated by structural covariance network of NAc in bipolar disorder and major depressive disorder. Progress in neuro-psychopharmacology & biological psychiatry *99*, 109865.

Hill, A.S., Sahay, A., and Hen, R. (2015). Increasing adult hippocampal neurogenesis is sufficient to reduce anxiety and depression-like behaviors. Neuropsychopharmacology *40*, 2368-2378.

Holm, M.M., Nieto-Gonzalez, J.L., Vardya, I., Henningsen, K., Jayatissa, M.N., Wiborg, O., and Jensen, K. (2011). Hippocampal GABAergic dysfunction in a rat chronic mild stress model of depression. Hippocampus *21*, 422-433.

Jakobs, M., Fomenko, A., Lozano, A.M., and Kiening, K.L. (2019). Cellular, molecular, and clinical mechanisms of action of deep brain stimulation-a systematic review on established indications and outlook on future developments. EMBO molecular medicine *11*.

Jones, J.L., Day, J.J., Wheeler, R.A., and Carelli, R.M. (2010). The basolateral amygdala differentially regulates conditioned neural responses within the nucleus accumbens core and shell. Neuroscience *169*, 1186-1198.

Khalid, A., Kim, B.S., Seo, B.A., Lee, S.T., Jung, K.H., Chu, K., Lee, S.K., and Jeon, D. (2016). Gamma oscillation in functional brain networks is involved in the spontaneous remission of depressive behavior induced by chronic restraint stress in mice. BMC neuroscience *17*, 4.

Lee, P.S., Chen, Y.S., Hsieh, J.C., Su, T.P., and Chen, L.F. (2010). Distinct neuronal oscillatory responses between patients with bipolar and unipolar disorders: a magnetoencephalographic study. J Affect Disord *123*, 270-275.

Li, Z., Chen, Z., Fan, G., Li, A., Yuan, J., and Xu, T. (2018). Cell-Type-Specific Afferent Innervation of the Nucleus Accumbens Core and Shell. Frontiers in neuroanatomy *12*, 84.

Lim, L.W., Janssen, M.L., Kocabicak, E., and Temel, Y. (2015a). The antidepressant effects of ventromedial prefrontal cortex stimulation is associated with neural activation in the medial part of the subthalamic nucleus. Behav Brain Res *279*, 17-21.

Lim, L.W., Prickaerts, J., Huguet, G., Kadar, E., Hartung, H., Sharp, T., and Temel, Y. (2015b). Electrical stimulation alleviates depressive-like behaviors of rats: investigation of brain targets and potential mechanisms. Transl Psychiatry *5*, e535.

Liu, C.H., Yang, M.H., Zhang, G.Z., Wang, X.X., Li, B., Li, M., Woelfer, M., Walter, M., and Wang, L. (2020). Neural networks and the anti-inflammatory effect of transcutaneous auricular vagus nerve stimulation in depression. Journal of neuroinflammation *17*, 54.

Liu, T.Y., Chen, Y.S., Su, T.P., Hsieh, J.C., and Chen, L.F. (2014). Abnormal early gamma responses to emotional faces differentiate unipolar from bipolar disorder patients. BioMed research international *2014*, 906104.

Liu, Y.Y., Liu, L., Zhu, L., Yang, X., Tong, K., You, Y., Yang, L., Gao, Y., Li, X., Chen, D.S., *et al.* (2021). dCA1-NAc shell glutamatergic projection mediates context-induced memory recall of morphine. Pharmacol Res *172*, 105857.

Malberg, J.E., Eisch, A.J., Nestler, E.J., and Duman, R.S. (2000). Chronic antidepressant treatment increases neurogenesis in adult rat hippocampus. Journal of Neuroscience *20*, 9104-9110.

Martisova, E., Solas, M., Horrillo, I., Ortega, J.E., Meana, J.J., Tordera, R.M., and Ramírez, M.J. (2012). Long lasting effects of early-life stress on glutamatergic/GABAergic circuitry in the rat hippocampus. Neuropharmacology *62*, 1944-1953.

Mayberg, H.S., Lozano, A.M., Voon, V., McNeely, H.E., Seminowicz, D., Hamani, C., Schwalb, J.M., and Kennedy, S.H. (2005). Deep brain stimulation for treatment-resistant depression. Neuron *45*, 651-660.

Minichino, A., Bersani, F.S., Capra, E., Pannese, R., Bonanno, C., Salviati, M., Delle Chiaie, R., and Biondi, M. (2012). ECT, rTMS, and deepTMS in pharmacoresistant drug-free patients with unipolar depression: a comparative review. Neuropsychiatric disease and treatment *8*, 55-64.

Miranda-Barrientos, J., Chambers, I., Mongia, S., Liu, B., Wang, H.L., Mateo-Semidey, G.E., Margolis, E.B., Zhang, S., and Morales, M. (2021). Ventral tegmental area GABA, glutamate, and glutamate-GABA neurons are heterogeneous in their electrophysiological and pharmacological properties. The European journal of neuroscience.

Möhler, H. (2012). The GABA system in anxiety and depression and its therapeutic potential. Neuropharmacology *62*, 42-53.

Mrazek, D.A., Hornberger, J.C., Altar, C.A., and Degtiar, I. (2014). A review of the clinical, economic, and societal burden of treatment-resistant depression: 1996-2013. Psychiatric services (Washington, DC) *65*, 977-987.

Nestler, E.J., and Carlezon, W.A., Jr. (2006). The mesolimbic dopamine reward circuit in depression. Biol Psychiatry *59*, 1151-1159.

Noda, Y., Zomorrodi, R., Saeki, T., Rajji, T.K., Blumberger, D.M., Daskalakis, Z.J., and Nakamura, M. (2017). Resting-state EEG gamma power and theta-gamma coupling enhancement following high-frequency left dorsolateral prefrontal rTMS in patients with depression. Clinical neurophysiology : official journal of the International Federation of Clinical Neurophysiology *128*, 424-432.

Ntamati, N.R., and Lüscher, C. (2016). VTA Projection Neurons Releasing GABA and Glutamate in the Dentate Gyrus. eNeuro *3*.

Nugent, A.C., Ballard, E.D., Gilbert, J.R., Tewarie, P.K., Brookes, M.J., and Zarate, C.A., Jr. (2020). The Effect of Ketamine on Electrophysiological Connectivity in Major Depressive Disorder. Frontiers in psychiatry *11*, 519.

Nullmeier, S., Panther, P., Dobrowolny, H., Frotscher, M., Zhao, S., Schwegler, H., and Wolf, R. (2011). Region‐specific alteration of GABAergic markers in the brain of heterozygous reeler mice. European Journal of Neuroscience *33*, 689-698.

Otte, C., Gold, S.M., Penninx, B.W., Pariante, C.M., Etkin, A., Fava, M., Mohr, D.C., and Schatzberg, A.F. (2016). Major depressive disorder. Nature reviews Disease primers *2*, 16065.

Pathak, Y., Salami, O., Baillet, S., Li, Z., and Butson, C.R. (2016). Longitudinal Changes in Depressive Circuitry in Response to Neuromodulation Therapy. Frontiers in neural circuits *10*, 50.

Perić, I., Stanisavljević, A., Inta, D., Gass, P., Lang, U.E., Borgwardt, S., and Filipović, D. (2019). Tianeptine antagonizes the reduction of PV+ and GAD67 cells number in dorsal hippocampus of socially isolated rats. Progress in Neuro-Psychopharmacology and Biological Psychiatry *89*, 386-399.

Rummel, J., Voget, M., Hadar, R., Ewing, S., Sohr, R., Klein, J., Sartorius, A., Heinz, A., Mathé, A.A., Vollmayr, B.*, et al.* (2016). Testing different paradigms to optimize antidepressant deep brain stimulation in different rat models of depression. Journal of psychiatric research *81*, 36-45.

Sauer, J.F., Strüber, M., and Bartos, M. (2015). Impaired fast-spiking interneuron function in a genetic mouse model of depression. Elife *4*.

Schlaepfer, T.E., Cohen, M.X., Frick, C., Kosel, M., Brodesser, D., Axmacher, N., Joe, A.Y., Kreft, M., Lenartz, D., and Sturm, V. (2008). Deep brain stimulation to reward circuitry alleviates anhedonia in refractory major depression. Neuropsychopharmacology *33*, 368-377.

Shaw, A.D., Saxena, N., L, E.J., Hall, J.E., Singh, K.D., and Muthukumaraswamy, S.D. (2015). Ketamine amplifies induced gamma frequency oscillations in the human cerebral cortex. European neuropsychopharmacology : the journal of the European College of Neuropsychopharmacology *25*, 1136-1146.

Song, J., Sun, J., Moss, J., Wen, Z., Sun, G.J., Hsu, D., Zhong, C., Davoudi, H., Christian, K.M., Toni, N.*, et al.* (2013). Parvalbumin interneurons mediate neuronal circuitry-neurogenesis coupling in the adult hippocampus. Nat Neurosci *16*, 1728-1730.

Song, J., Zhong, C., Bonaguidi, M.A., Sun, G.J., Hsu, D., Gu, Y., Meletis, K., Huang, Z.J., Ge, S., and Enikolopov, G. (2012). Neuronal circuitry mechanism regulating adult quiescent neural stem-cell fate decision. Nature *489*, 150-154.

Strelets, V.B., Garakh Zh, V., and Novototskii-Vlasov, V.Y. (2007). Comparative study of the gamma rhythm in normal conditions, during examination stress, and in patients with first depressive episode. Neuroscience and behavioral physiology *37*, 387-394.

Tendolkar, I., van Beek, M., van Oostrom, I., Mulder, M., Janzing, J., Voshaar, R.O., and van Eijndhoven, P. (2013). Electroconvulsive therapy increases hippocampal and amygdala volume in therapy refractory depression: a longitudinal pilot study. Psychiatry research *214*, 197-203.

Tunc-Ozcan, E., Peng, C.Y., Zhu, Y., Dunlop, S.R., Contractor, A., and Kessler, J.A. (2019). Activating newborn neurons suppresses depression and anxiety-like behaviors. Nature communications *10*, 3768.

Vaden, R.J., Gonzalez, J.C., Tsai, M.C., Niver, A.J., Fusilier, A.R., Griffith, C.M., Kramer, R.H., Wadiche, J.I., and Overstreet-Wadiche, L. (2020). Parvalbumin interneurons provide spillover to newborn and mature dentate granule cells. Elife *9*.

Wacker, J., Dillon, D.G., and Pizzagalli, D.A. (2009). The role of the nucleus accumbens and rostral anterior cingulate cortex in anhedonia: integration of resting EEG, fMRI, and volumetric techniques. NeuroImage *46*, 327-337.

Wang, J., Tang, J., Liang, X., Luo, Y., Zhu, P., Li, Y., Xiao, K., Jiang, L., Yang, H., Xie, Y., *et al.* (2021). Hippocampal PGC-1α-mediated positive effects on parvalbumin interneurons are required for the antidepressant effects of running exercise. Transl Psychiatry *11*, 222.

Williams, N.R., Bentzley, B.S., Hopkins, T., Pannu, J., Sahlem, G.L., Takacs, I., George, M.S., Nahas, Z., and Short, E.B. (2018). Optimization of epidural cortical stimulation for treatment-resistant depression. Brain stimulation *11*, 239-240.

Xia, Y., Driscoll, J.R., Wilbrecht, L., Margolis, E.B., Fields, H.L., and Hjelmstad, G.O. (2011). Nucleus accumbens medium spiny neurons target non-dopaminergic neurons in the ventral tegmental area. Journal of Neuroscience *31*, 7811-7816.

Yi, Y., Song, Y., and Lu, Y. (2020). Parvalbumin Interneuron Activation-Dependent Adult Hippocampal Neurogenesis Is Required for Treadmill Running to Reverse Schizophrenia-Like Phenotypes. Frontiers in cell and developmental biology *8*, 24.

Zhang, H., He, X., Mei, Y., and Ling, Q. (2018). Ablation of ErbB4 in parvalbumin-positive interneurons inhibits adult hippocampal neurogenesis through down-regulating BDNF/TrkB expression. The Journal of comparative neurology *526*, 2482-2492.

Zhou, C., Zhang, H., Qin, Y., Tian, T., Xu, B., Chen, J., Zhou, X., Zeng, L., Fang, L., and Qi, X. (2018). A systematic review and meta-analysis of deep brain stimulation in treatment-resistant depression. Progress in Neuro-Psychopharmacology and Biological Psychiatry *82*, 224-232.

Zou, D., Chen, L., Deng, D., Jiang, D., Dong, F., McSweeney, C., Zhou, Y., Liu, L., Chen, G., and Wu, Y. (2016). DREADD in parvalbumin interneurons of the dentate gyrus modulates anxiety, social interaction and memory extinction. Current molecular medicine *16*, 91-102.

13. Figure and captions

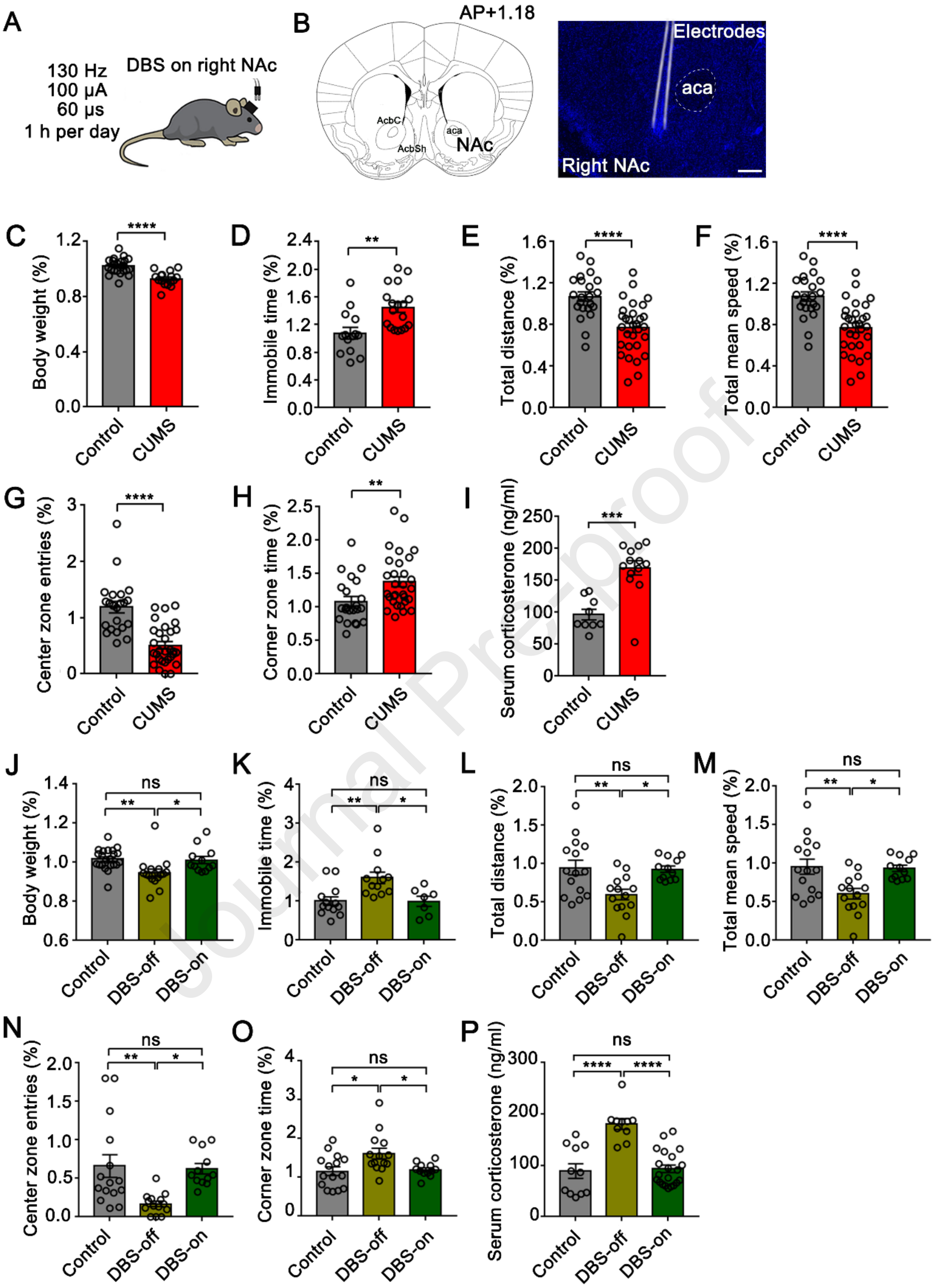

Fig. 1. DBS treatment rescued the depression-like behaviors induced by CUMS.

(A-B) The stimulation electrode (bipolar, two parallel tungsten wires, 0.22 mm in diameter) was implanted at the right AcbC of the mouse. The electrical stimulation (130 Hz, 100 μA, and 60 μs pulse width) was given 1 h per day for 7 days. NAc, accumbens nucleus; AcbC, accumbens nucleus core; AcbSh, accumbens nucleus shell; aca, anterior commissure. Scale bar, 200 μm.

(C) The body weight decreased in the depression group (Unpaired *t*-test, $t = 5.081$, df = 36, $p < 0.0001$. n = 22 and 16 in control and CUMS groups, respectively).

(D) The immobile time in TST increased in the depression group (Unpaired *t*-test, $t = 3.365$, df = 30, $p = 0.0021$. n = 14 and 18 in control and CUMS groups, respectively).

(E-H) CUMS treatment reduced locomotion activity and induced anxiety-like behavior, revealed by OFT (n = 22 and 30 in control and CUMS groups, respectively, Unpaired *t*-test). The total distance traveled decreased (E, $t = 4.601$, df = 50, $p < 0.0001$), the mean velocity decreased (F, $t = 4.599$, df = 50, $p < 0.0001$), the center zone entries decreased (G, $t = 5.899$, df = 50, $p < 0.0001$), and the corner zone time increased in CUMS group (H, $t = 2.754$, df = 50, $p = 0.0082$).

(I) Serum corticosterone concentration increased in CUMS group (Unpaired *t*-test, $t = 4.793$, df = 20, $p = 0.0001$. n = 9 and 13 in control and CUMS groups, respectively).

(J) DBS reversed CUMS-induced body weight loss (One-way ANOVA, $F(2, 47) = 6.194$, $p = 0.0041$; Tukey's *post hoc* test: Control vs. DBS-off, $p = 0.0048$; DBS-off vs. DBS-on, $p = 0.0283$; Control vs. DBS-on, $p = 0.9748$. n = 22, 16 and 12 in control, DBS-off and DBS-on groups, respectively.)

(K) DBS reversed CUMS-induced immobile time increase in the tail suspension test (One-way ANOVA, $F(2, 29) = 7.146$, $p = 0.003$; Tukey's *post hoc* test: Control vs. DBS-off, $p = 0.005$; DBS-off vs. DBS-on, $p = 0.0176$; Control vs. DBS-on, $p = 0.9992$. n = 13, 12 and 7 in control, DBS-off and DBS-on groups, respectively).

(L-O) DBS treatment promoted locomotion activity and improved anxiety-like behavior, revealed by OFT (n = 15, 14, and 12 in control, DBS-off, and DBS-on groups, respectively, One-way ANOVA). DBS reversed CUMS-induced the total distance decrease (L, $F(2, 38) = 6.731$, $p = 0.0031$; Tukey's *post hoc* test: Control vs. DBS-off, $p = 0.0054$; DBS-off vs. DBS-on, $p = 0.014$; Control vs. DBS-on, $p = 0.9819$). DBS reversed CUMS-induced the mean velocity decrease (M, $F(2, 38) = 6.788$, $p = 0.003$; Tukey's *post hoc* test: Control vs. DBS-off, $p = 0.005$; DBS-off vs. DBS-on, $p = 0.0139$; Control vs. DBS-on, $p = 0.9778$). DBS reversed CUMS-induced center zone entries decrease (N, $F(2, 38) = 7.435$, $p = 0.0019$; Tukey's *post hoc* test: Control vs. DBS-off, $p = 0.0032$; DBS-off vs. DBS-on, $p = 0.01$; Control vs. DBS-on, $p = 0.9711$). DBS reversed CUMS-induced corner zone time increase (O, $F(2, 38) = 5.395$, $p = 0.0087$; Tukey's *post hoc* test: Control vs. DBS-off, $p = 0.0123$; DBS-off vs. DBS-on, $p = 0.034$; Control vs. DBS-on, $p = 0.9665$).

(P) DBS reversed CUMS-induced the serum corticosterone concentration increase (One-way ANOVA, $F(2, 39) = 21.29$, $p < 0.0001$; Tukey's *post hoc* test: Control vs. DBS-off, $p < 0.0001$; DBS-off vs. DBS-on, $p < 0.0001$; Control vs. DBS-on, $p = 0.9528$. n = 11, 10 and 21 in control, DBS-off and DBS-on groups, respectively).

Data are expressed as mean ± SEM. * $p < 0.05$， ** $p < 0.01$, *** $p < 0.001$, ****$p < 0.0001$.

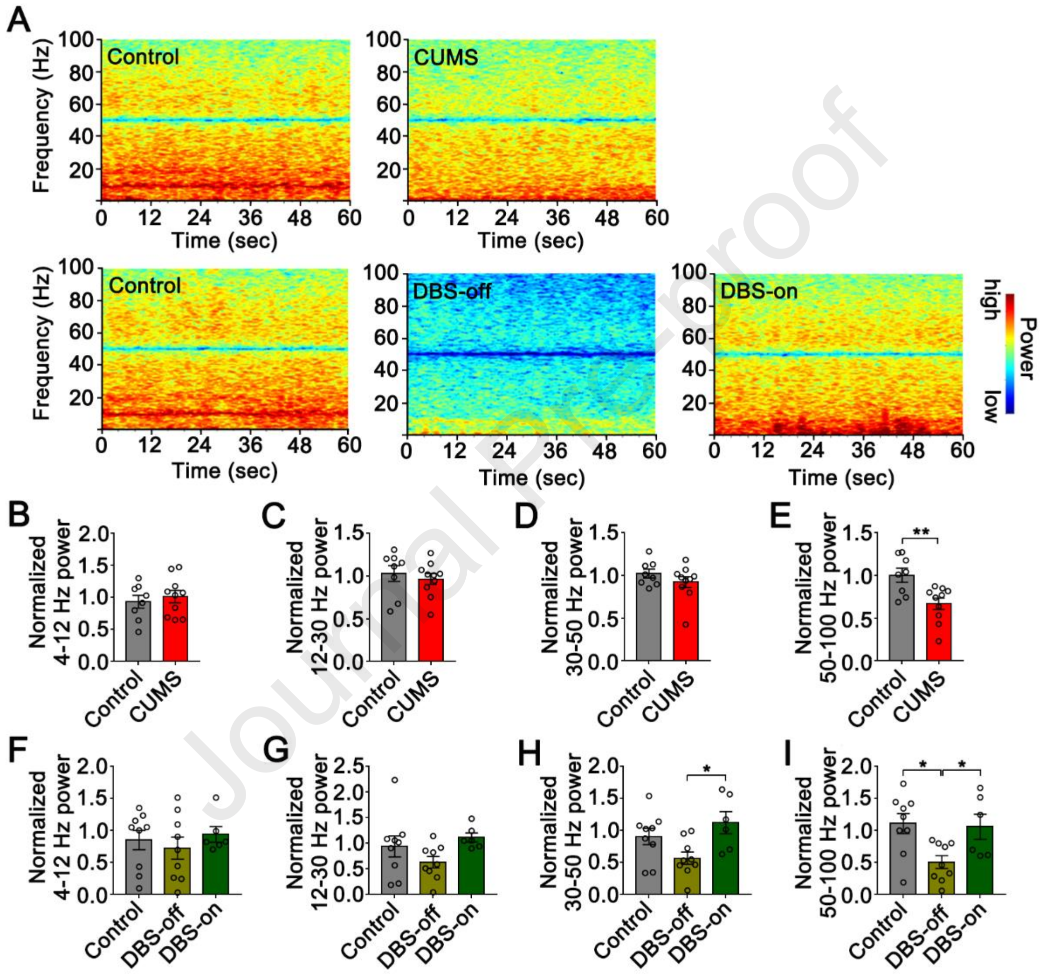

Fig. 2. DBS reversed CUMS-induced high gamma oscillation reduction in the dorsal DG.

(A) Spectrograms of representative LFP in the dorsal DG of mice in the home cage. Color codes indicate LFP powers of the frequency spectrum.

(B-D) Chronic stress did not affect Theta oscillation (B, Unpaired *t*-test, $t = 0.7999$, df = 16, $p = 0.4355$), Beta oscillation (C, Unpaired *t*-test, $t = 0.04209$, df = 16, $p = 0.9669$), Low gamma oscillation (D, Unpaired *t*-test, $t = 1.18$, df = 16, $p = 0.2554$) in the dorsal DG of mice after CUMS in the home cage (n = 8 and 10 in control and CUMS groups, respectively).

(E) High gamma oscillation power was decreased in the dorsal DG of depressed mice after CUMS in the home cage (Unpaired *t*-test, $p = 0.0054$. n = 8 and 10 in control and depression groups, respectively).

(F-H) DBS treatment caused neuronal oscillation changes in the dorsal DG in home cage (n = 9, 9 and 6 in control, DBS-off and DBS-on groups, respectively). (F) Theta oscillation (One-way ANOVA, $F(2, 21) = 0.4358$, $p = 0.6524$). (G) Beta oscillation (One-way ANOVA, $F(2, 21) = 2.307$, $p = 0.1242$). (H) Low gamma oscillation (One-way ANOVA, $F(2, 21) = 4.542$, $p =0.0229$; Tukey's *post hoc* test: DBS-off vs. DBS-on, $p = 0.0216$).

(I) The DBS treatment reversed CUMS-induced high gamma oscillation power decrease in the dorsal DG in the home cage (One-way ANOVA, $F(2, 21) = 5.577$, $p = 0.0114$; Tukey's *post hoc* test: Control vs. DBS-off, $p = 0.0149$; DBS-off vs. DBS-on, $p = 0.0493$; Control vs. DBS-on, $p = 0.9714$. n = 9, 9 and 6 in control, DBS-off, and DBS-on groups, respectively).

Data are expressed as mean ± SEM. * $p < 0.05$, ** $p < 0.01$.

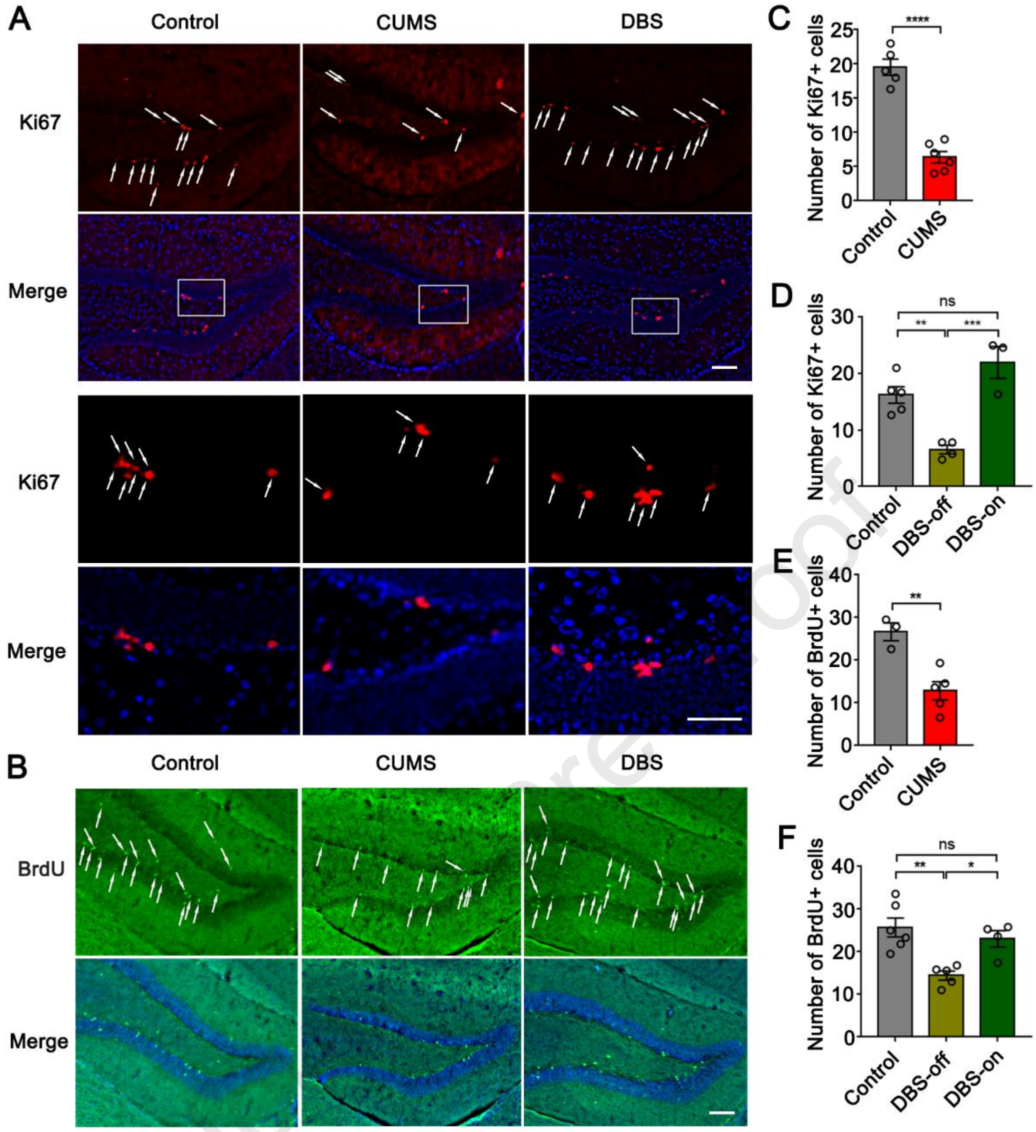

Fig. 3. DBS treatment increased adult neurogenesis in the dorsal DG of the CUMS-induced depression-like mouse model.

(A) Representative photomicrographs showing Ki67-positive cells in the DG. Upper plate, scale bar, 100 μm. Below plate, scale bar, 50 μm.

(B) Representative photomicrographs showing BrdU-positive cells in the DG. Scale bar, 100 μm.

(C) Quantitative analysis of the number of Ki67-positive cells in the DG of the CUMS-induced depression-like mice. Five sections at least in each animal were picked and analyzed (Unpaired *t*-test, $t = 9.251$, df = 9, $p < 0.0001$. n = 5 and 6 in control and depression groups, respectively).

(D) Quantitative analysis of the number of Ki67-positive cells in the DG of DBS treatment mice. (One-way ANOVA, $F(2, 9) = 20.09$, $p < 0.0005$; Tukey's *post hoc* test: Control vs. DBS-off, $p = 0.0046$; DBS-off vs. DBS-on, $p = 0.0004$; Control vs. DBS-on, $p = 0.0912$. n = 5, 4 and 3 in control, DBS-off and DBS-on groups, respectively).

(E) Quantitative analysis of the number of BrdU-positive cells in the DG of the CUMS-induced depression-like mice. (Unpaired *t*-test, $t = 4.25$, df = 6, $p = 0.0054$. n = 3 and 5 in control and depression groups, respectively).

(F) Quantitative analysis of the number of BrdU-positive cells in the DG of DBS treatment mice (One-way ANOVA, $F(2, 12) = 10.08$, $p = 0.0027$; Tukey's *post hoc* test: Control vs. DBS-off, $p = 0.0024$; DBS-off vs. DBS-on, $p = 0.0266$; Control vs. DBS-on, $p = 0.6114$. n = 6, 5 and 4 in control, DBS-off and DBS-on groups, respectively).

Data are expressed as mean ± SEM. * $p < 0.05$， ** $p < 0.01$， *** $p < 0.001$, **** $p < 0.0001$.

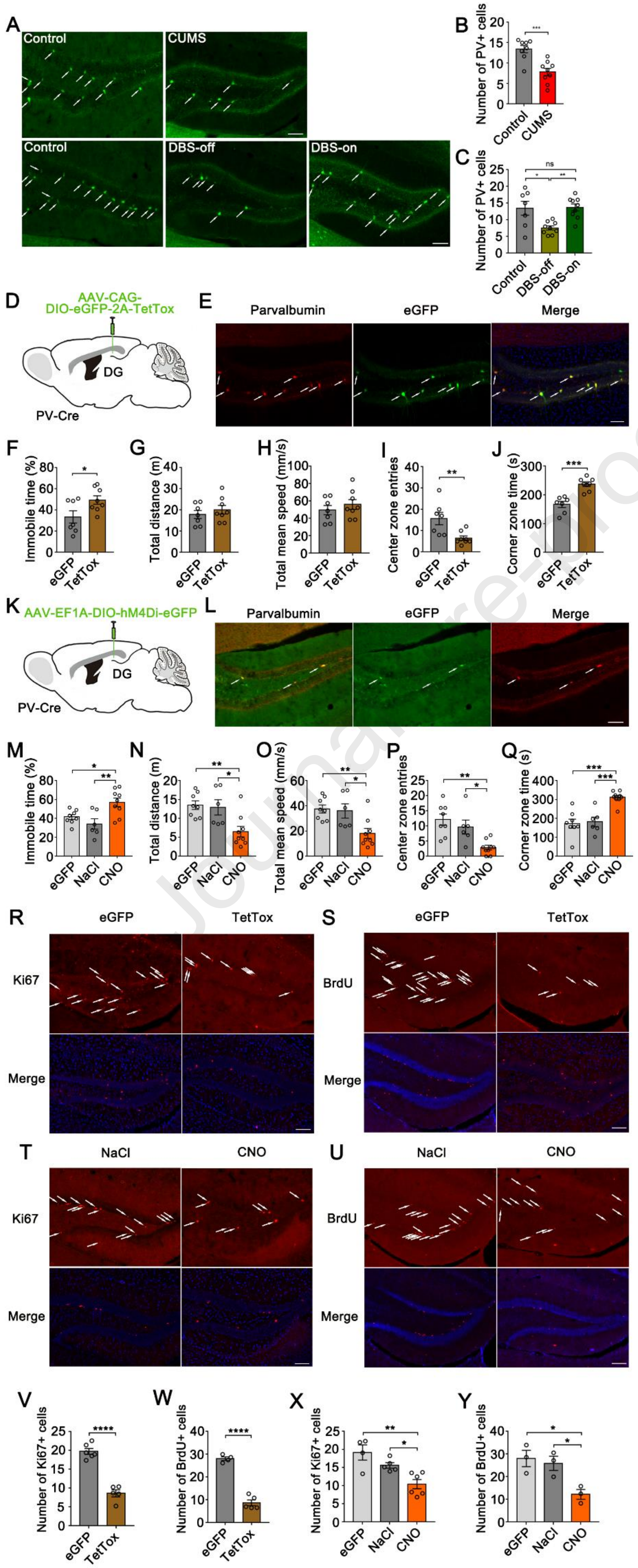

A
Control
CUMS
Control
DBS-off
DBS-on
B
Number of PV+ cells
Control
CUMS
C
ns
Number of PV+ cells
Control
DBS-off
DBS-on
D
AAV-CAG-
DIO-eGFP-2A-TetTox
DG
PV-Cre
E
Parvalbumin
eGFP
Merge
F
Immobile time (%)
G
Total distance (m)
H
Total mean speed (mm/s)
I
Center zone entries
J
Corner zone time (s)
eGFP
TetTox
K
AAV-EF1A-DIO-hM4Di-eGFP
DG
PV-Cre
L
Parvalbumin
eGFP
Merge
M
N
O
P
Q
eGFP
NaCl
CNO
R
eGFP
TetTox
Ki67
Merge
S
eGFP
TetTox
BrdU
Merge
T
NaCl
CNO
Ki67
Merge
U
NaCl
CNO
BrdU
Merge
V
Number of Ki67+ cells
W
Number of BrdU+ cells
X
Number of Ki67+ cells
Y
Number of BrdU+ cells

Fig. 4. Inhibition of PVI in the dorsal DG induced depression-like behaviors and decreased newborn cells.

(A) Representative photomicrographs showing PVI in the dorsal DG. Scale bar, 100 μm.

(B) The number of PVI decreased in the dorsal DG after CUMS treatment. (Unpaired *t*-test, t = 4.366, df = 15, p = 0.0006. n = 8 and 9 in control and CUMS groups, respectively).

(C) The number of PVI was reversed in the dorsal DG after DBS treatment (One-way ANOVA, F(2, 22) = 7.973, p = 0.0025; Tukey's *post hoc* test: Control vs. DBS-off, p = 0.0103; DBS-off vs. DBS-on, p = 0.0045; Control vs. DBS-on, p = 0.9917. n = 7, 9, and 9 in control, DBS-off, and DBS-on groups, respectively).

(D) Schematic illustration of AAV-CAG-DIO-eGFP-2A-TetTox injection in the dorsal DG of PV-Cre mice.

(E) TetTox/eGFP neurons (green) in the dorsal DG co-expressed PV (red); scale bar, 100 μm.

(F) The immobile time in the tail suspension test increased in the PV-TetTox mice group (Unpaired *t*-test, t = 2.321, df = 13, p = 0.0371. n = 7 and 8 in PV-eGFP mice and PV-TetTox mice groups, respectively).

(G-J) Inhibition of PVI in the dorsal DG induced anxiety-like behaviors, revealed by OFT (n = 7 and 8 in PV-eGFP mice and PV-TetTox mice groups, respectively, Unpaired *t*-test). The total distance (G, t = 0.8144, df = 13, p =0.4301), the mean velocity decreased (H, t = 0.8155, df = 13, p = 0.4295), the center zone entries decreased in PV-TetTox mice group (I, t = 3.149, df = 13, p = 0.0077), the corner zone time increased in PV-TetTox mice group (J, t = 5.497, df = 13, p = 0.0001).

(K) Schematic illustration of AAV-EF1A-DIO-hM4Di-eGFP injection in the dorsal DG of PV-Cre mice.

(L) hM4Di-eGFP neurons (green) in DG co-expressed PV (red); scale bar, 100 μm.

(M) The immobile time in the tail suspension test increased in the CNO group (One-way ANOVA, F(2, 20) = 7.328, p = 0.0041; Tukey's *post hoc* test: eGFP vs. CNO, p = 0.0376; NaCl vs. CNO, p = 0.0045; eGFP vs. NaCl, p = 0.4999. n = 8, 6, and 9 in eGFP, NaCl, and CNO groups, respectively).

(N-Q) Chemogenetic inhibition of PVI in the dorsal DG reduced locomotion activity and induced anxiety-like behavior, revealed by OFT (n = 8, 6, and 9 in eGFP, NaCl, and CNO groups, respectively, One-way ANOVA). The total distance traveled decreased in the CNO group (N, F(2, 20) = 7.501, p = 0.0037; Tukey's *post hoc* test: eGFP vs. CNO, p = 0.0058; NaCl vs. CNO, p =

0.0195; eGFP vs. NaCl, $p = 0.9625$), the mean velocity decreased in the CNO group (O, $F(2, 20) = 7.5$, $p = 0.0037$; Tukey's *post hoc* test: eGFP vs. CNO, $p = 0.0058$; NaCl vs. CNO, $p = 0.0195$; eGFP vs. NaCl, $p = 0.9624$), the center zone entries decreased in the CNO group (P, $F(2, 20) = 9.71$ $p = 0.0011$; Tukey's *post hoc* test: eGFP vs. CNO, $p = 0.0011$; NaCl vs. CNO, $p = 0.0241$; eGFP vs. NaCl, $p = 0.5738$), the corner zone time increased in the CNO group (Q, $F(2, 20) = 17$, $p < 0.0001$; Tukey's *post hoc* test: eGFP vs. CNO, $p = 0.0001$; NaCl vs. CNO, $p = 0.0006$; eGFP vs. NaCl, $p = 0.9487$).

(R) Representative photomicrographs showing Ki67 positive cells in the dorsal DG of PV-TetTox mice. Scale bar, 100 µm.

(S) Representative photomicrographs showing BrdU positive cells in the dorsal DG of PV-TetTox mice. Scale bar, 100 µm.

(T) Representative photomicrographs showing Ki67 positive cells in the dorsal DG of PV-hM4Di mice. Scale bar, 100 µm.

(U) Representative photomicrographs showing BrdU positive cells in the dorsal DG of PV-hM4Di mice. Scale bar, 100 µm.

(V) Quantitative analysis of the number of Ki67-positive cells in the dorsal DG of PV-TetTox mice (Unpaired *t*-test, $t = 9.188$, df = 9, $p < 0.0001$. n = 6 and 5 in PV-eGFP mice and PV-TetTox mice groups, respectively).

(W) Quantitative analysis of the number of BrdU-positive cells in the dorsal DG of PV-TetTox mice (Unpaired *t*-test, $t = 11.99$, df = 7, $p < 0.0001$. n = 4 and 5 in PV-eGFP mice and PV-TetTox mice groups, respectively).

(X) Quantitative analysis of the number of Ki67-positive cells in the dorsal DG of PV-hM4Di mice (One-way ANOVA, $F(2, 12) = 10.25$, $p = 0.0025$; Tukey's *post hoc* test: eGFP vs. CNO, $p = 0.0022$; NaCl vs. CNO, $p = 0.0408$; eGFP vs. NaCl, $p = 0.2314$. n = 4, 5, and 6 in eGFP, NaCl, and CNO groups, respectively).

(Y) Quantitative analysis of the number of BrdU-positive cells in the dorsal DG of PV-hM4Di mice (One-way ANOVA, $F(2, 6) = 8.057$, $p = 0.02$; Tukey's *post hoc* test: eGFP vs. CNO, $p = 0.0236$; NaCl vs. CNO, $p = 0.0424$; eGFP vs. NaCl, $p = 0.8763$. n = 3 in eGFP, NaCl, and CNO groups).

Data are expressed as mean ± SEM. * $p < 0.05$， ** $p < 0.01$, *** $p < 0.001$, **** $p < 0.0001$.

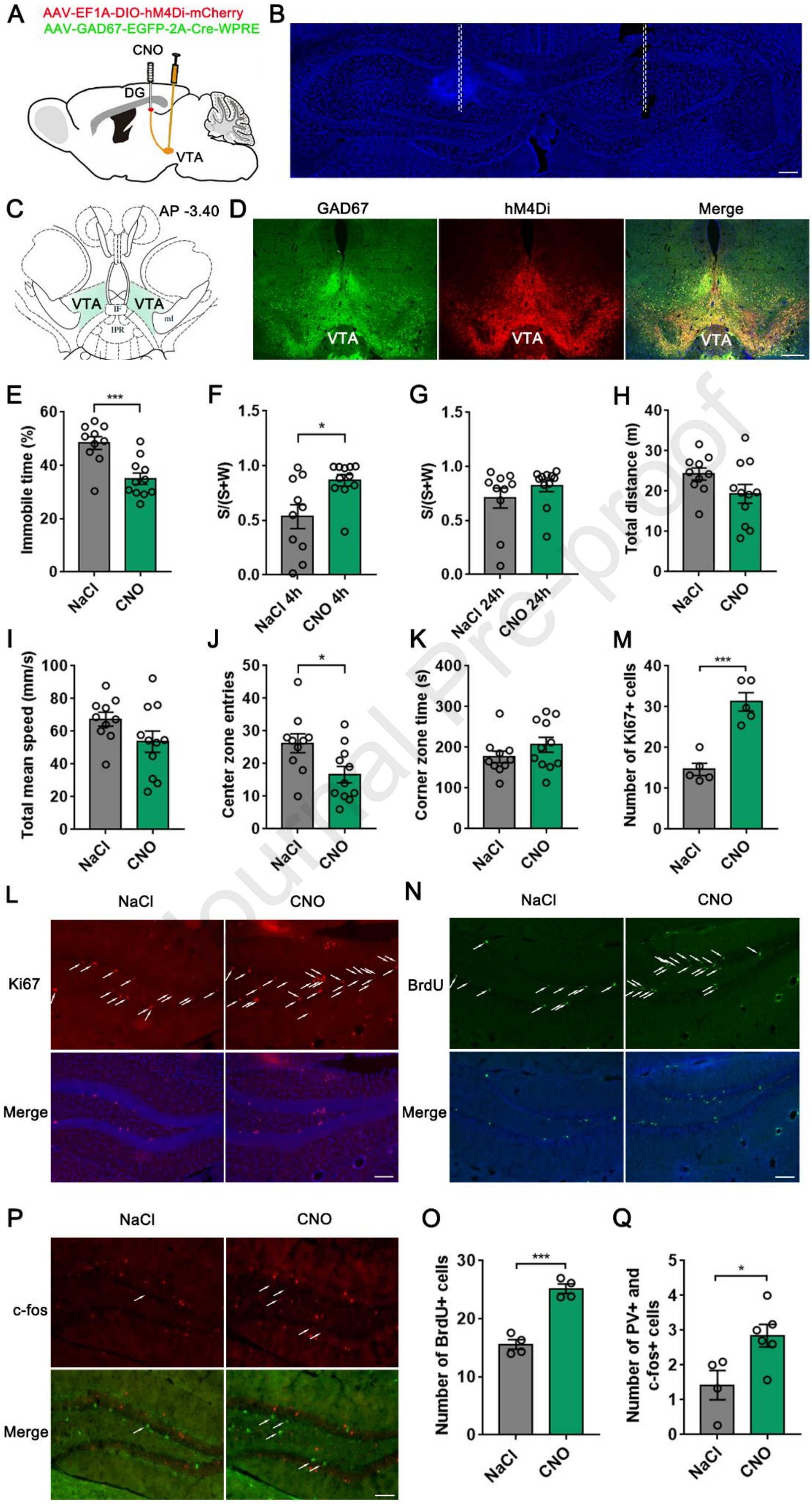
A
AAV-EF1A-DIO-hM4Di-mCherry
AAV-GAD67-EGFP-2A-Cre-WPRE
CNO
DG
VTA
B
C
AP -3.40
VTA
VTA
D
GAD67
hM4Di
Merge
E
Immobile time (%)
NaCl
CNO
F
S/(S+W)
NaCl 4h
CNO 4h
G
NaCl 24h
CNO 24h
H
Total distance (m)
I
Total mean speed (mm/s)
J
Center zone entries
K
Corner zone time (s)
M
Number of Ki67+ cells
L
Ki67
Merge
N
BrdU
P
c-fos
O
Number of BrdU+ cells
Q
Number of PV+ and c-fos+ cells

Fig. 5 Inhibiting the projection of VTA-DG GABAergic neurons has an antidepressant effect.

(A) Schematic shows chemogenetic inhibition of VTA GABAergic afferents neurons in the DG.

(B) Schematic representation of the localization of the bilateral DG-injection of CNO. Scale bar, 200 μm.

(C) Schematic illustration of the VTA.

(D) Representative photomicrographs show viral of GAD67-Cre and hM4Di express in the VTA. Scale bar, 200 μm.

(E) The immobile time in the tail suspension test decreased in VTA^{GABA}-DG mice with the CNO group (Unpaired *t*-test, $t = 4.119$, df = 19, $p = 0.0006$. n = 10 and 11 in NaCl and CNO groups, respectively).

(F) The preference for the sucrose solution increased in VTA^{GABA}-DG mice with local injection of CNO within 4 hours (Unpaired *t*-test, $t = 2.81$, df = 19, $p = 0.0112$. n = 10 and 11 in NaCl and CNO groups, respectively).

(G) The VTA^{GABA}-DG mice with local injection of CNO within 24 hours displayed a similar preference for the sucrose solution compared to the VTA^{GABA}-DG mice with local injection of 0.9% NaCl (Unpaired *t*-test, $t = 1.088$, df = 19, $p = 0.2904$. n = 10 and 11 in NaCl and CNO groups, respectively).

(H-K) Chemogenetic inhibition of the projection of VTA-DG GABAergic neurons induced mild anxiety-like behavior, revealed by OFT (Unpaired *t*-test, n = 10 and 11 in NaCl and CNO groups, respectively). The total distance (H, $t = 1.723$, df = 19, $p = 0.1011$), the mean velocity (I, $t = 1.723$, df = 19, $p = 0.1012$), the center zone entries decreased in VTA^{GABA}-DG mice with the CNO group (J, $t = 2.497$, df = 19, $p = 0.0219$), and the corner zone time (K, $t = 1.269$, df = 19, $p = 0.2196$).

(L) Representative photomicrographs showing Ki67 positive cells in the dorsal DG of VTA^{GABA}-DG mice. Scale bar, 100 μm.

(M) Quantitative analysis of the number of Ki67 positive cells in the DG of VTA^{GABA}-DG mice. The number of Ki67-positive cells increased in the dorsal DG of VTA^{GABA}-DG mice with the CNO group (Unpaired *t*-test, $t = 6.094$, df = 8, $p = 0.0003$. n = 5 in NaCl and CNO groups).

(N) Representative photomicrographs showing BrdU positive cells in the DG of VTA^{GABA}-DG mice. Scale bar, 100 μm.

(O) Quantitative analysis of the number of BrdU positive cells in the DG of VTA^{GABA}-DG mice.

The number of BrdU -positive cells increased in the dorsal DG of VTA^{GABA}-DG mice with the CNO group (Unpaired *t*-test, $t = 8.129$, df = 6, $p = 0.0002$. n = 4 in NaCl and CNO groups).

(P) Representative photomicrographs showing c-fos and PVI co-expression cells in the DG of VTA^{GABA}-DG mice. Scale bar, 100 µm.

(Q) Quantitative analysis of the number of c-fos and PVI co-expression cells in the DG of VTA^{GABA}-DG mice. The number of c-fos and PVI co-expression cells increased in the dorsal DG of VTA^{GABA}-DG mice with the CNO group (Unpaired *t*-test, $t = 2.702$, df = 8, $p = 0.027$. n = 4 and 6 in NaCl and CNO groups, respectively).

Data are expressed as mean ± SEM. * $p < 0.05$, *** $p < 0.0001$.

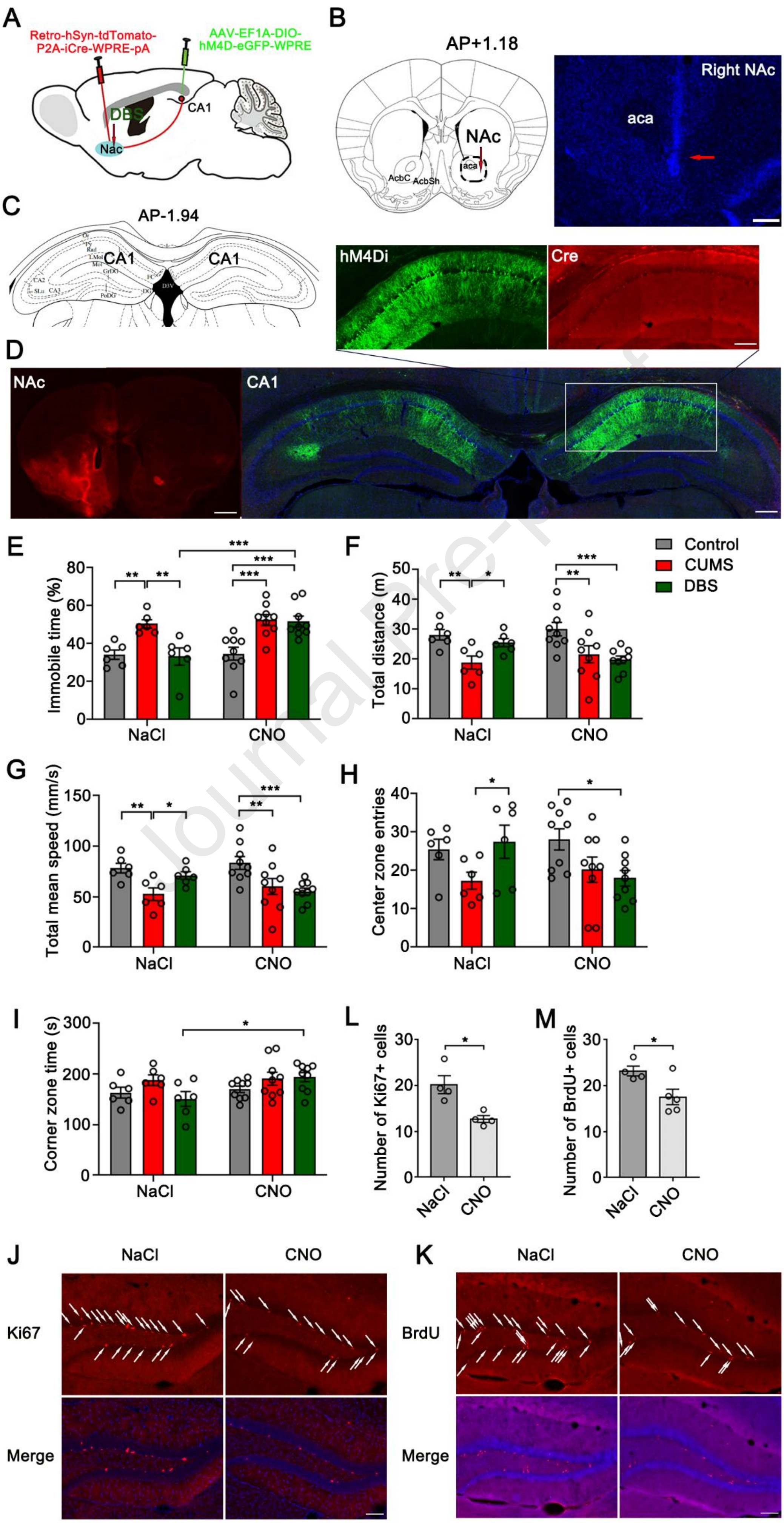
A
Retro-hSyn-tdTomato-P2A-iCre-WPRE-pA
AAV-EF1A-DIO-hM4D-eGFP-WPRE
DBS
CA1
Nac
B
AP+1.18
NAc
aca
AcbC
AcbSh
Right NAc
aca
C
AP-1.94
CA1
CA1
hM4Di
Cre
D
NAc
CA1
E
Immobile time (%)
NaCl
CNO
F
Total distance (m)
NaCl
CNO
Control
CUMS
DBS
G
Total mean speed (mm/s)
NaCl
CNO
H
Center zone entries
NaCl
CNO
I
Corner zone time (s)
NaCl
CNO
L
Number of Ki67+ cells
NaCl
CNO
M
Number of BrdU+ cells
NaCl
CNO
J
NaCl
CNO
Ki67
Merge
K
NaCl
CNO
BrdU
Merge

Fig. 6 Chemogenetic inhibition of CA1 projection to NAc affected the therapeutic effect of DBS-on depression.

(A) Schematic illustration of Retro-hSyn-tdTomato-P2A-iCre-WPRE-pA injection in NAc and pAAV-EF1A-DIO-hM4Di-eGFP-WPRE injection in CA1 to inhibit the projection of CA1 to NAc.

(B) The stimulation electrode was implanted at the right AcbC of the mouse (red arrow). Scale bar, 200 μm.

(C) Schematic illustration of the CA1.

(D) Representative photomicrographs showing viral of retro-iCre expression in the NAc (left, scale bar, 300 μm), retro-iCre and hM4Di expression in the CA1(right; top, scale bar, 150 μm; bottom, scale bar, 200 μm).

(E) CNO abolished the DBS treatment effect of reversing the immobile time increase in depression group (Two-way ANOVA, *post hoc* test: ** $p < 0.01$，*** $p < 0.001$. n = 6 and 9 in NaCl and CNO groups, respectively).

(F-I) CNO abolished the DBS treatment effect of reversing anxiety-like behaviors in depression group (Two-way ANOVA, *post hoc* test: * $p < 0.05$, ** $p < 0.01$，*** $p < 0.001$. n = 6 and 9 in NaCl and CNO groups, respectively). The total distance traveled decreased in DBS treatment with CNO group (F), the mean velocity decreased in DBS treatment with CNO group (G), the center zone entries decreased in DBS treatment with CNO group (H), the corner zone time increased in DBS treatment with CNO group (I).

(J) Representative photomicrographs showing Ki67 positive cells in the dorsal DG of DBS treatment with CNO group mice. Scale bar, 100 μm.

(K) Representative photomicrographs showing BrdU positive cells in the dorsal DG of DBS treatment with CNO group mice. Scale bar, 100 μm.

(L) The number of Ki67-positive cells decreased in the dorsal DG of DBS treatment with CNO group mice (Unpaired *t*-test, $t = 3.545$, df = 6, $p = 0.0121$. n = 4 and 4 in NaCl and CNO groups, respectively).

(M) The number of BrdU-positive cells decreased in the dorsal DG of DBS treatment with CNO group mice (Unpaired *t*-test, $t = 2.65$, df = 7, $p = 0.0329$. n = 4 and 5 in NaCl and CNO groups, respectively).

Data are expressed as mean ± SEM. * $p < 0.05$, ** $p < 0.01$，*** $p < 0.001$.

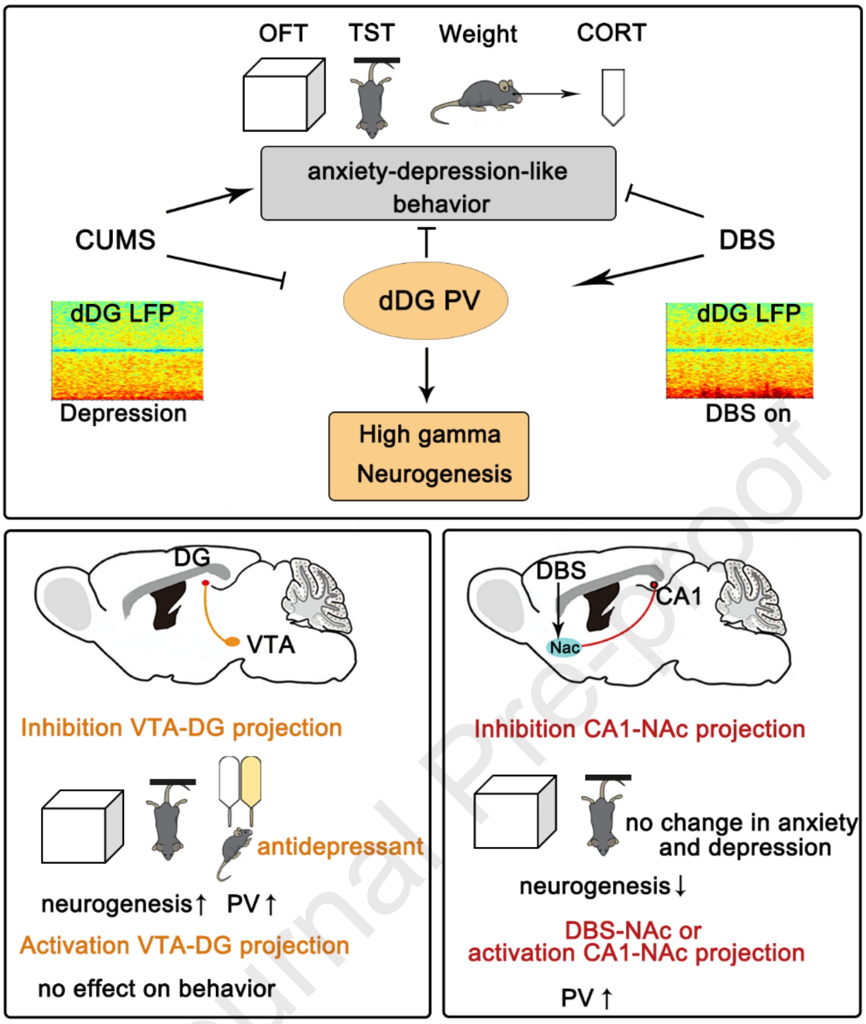

Fig.7. Summary of findings. The upper part: NAc-DBS treatment rescued depression-like behaviors induced by CUMS, reversed high gamma oscillation reduction, PV neuron loss, and neurogenesis impairment in the dorsal DG of depression mice. Chemogenetic inhibition of PV interneurons in the dorsal hippocampus led to depression-like behavior and decreased adult neurogenesis. The lower parts: the projection of VTA-DG (left) and CA1-NAc (right) may jointly participate in this therapeutic mechanism. Inhibition of the CA1-NAc projection reduced the antidepressant effect of DBS-NAc, while disinhibition of the VTA-DG GABAergic projection has an antidepressant effect. Activating the CA1-NAc projection or disinhibition of the VTA-DG GABAergic projection could increase PVI activity in the dorsal DG.

Conflict of Interest

The authors declare that there are no conflict of interests, we do not have any possible conflicts of interest.